

BONSAI: Bayesian Optimization with Natural Simplicity and Interpretability

Samuel Daulton¹ David Eriksson¹ Maximilian Balandat¹ Eytan Bakshy¹

Abstract

Bayesian optimization (BO) is a popular technique for sample-efficient optimization of black-box functions. In many applications, the parameters being tuned come with a carefully engineered default configuration, and practitioners only want to deviate from this default when necessary. Standard BO, however, does not aim to minimize deviation from the default and, in practice, often pushes weakly relevant parameters to the boundary of the search space. This makes it difficult to distinguish between important and spurious changes and increases the burden of vetting recommendations when the optimization objective omits relevant operational considerations. We introduce BONSAI, a default-aware BO policy that prunes low-impact deviations from a default configuration while explicitly controlling the loss in acquisition value. BONSAI is compatible with a variety of acquisition functions, including expected improvement and upper confidence bound (GP-UCB). We theoretically bound the regret incurred by BONSAI, showing that, under certain conditions, it enjoys the same no-regret property as vanilla GP-UCB. Across many real-world applications, we empirically find that BONSAI substantially reduces the number of non-default parameters in recommended configurations while maintaining competitive optimization performance, with little effect on wall time.

1. Introduction

Bayesian optimization (BO) (Garnett, 2023) has become a popular approach for optimizing expensive and noisy black-box functions, with applications ranging from hyperparameter tuning to physical experiment design and system configuration. BO relies on a probabilistic surrogate model of an unknown objective f , which is used in an acquisition function to select informative points to evaluate next.

¹Meta. Correspondence to: Samuel Daulton <sdaulon@meta.com>.

In many of these applications, there is a distinguished *default* or *status quo* configuration. For instance, production systems often ship with carefully tuned configurations, compiler flags, or model-serving infrastructure. Deviating from such defaults can be costly: changing many parameters at once can introduce unintended behaviors that are not captured in the optimization objective and can increase technical debt (Sculley et al., 2015; Liu et al., 2023).

Practitioners, therefore, frequently ask a question that standard BO does not address directly: “*Given a current default configuration, what is the minimal set of changes I can make to optimize my system?*” Unfortunately, conventional BO is indifferent to this preference; it typically adjusts many weakly relevant parameters and often pushes marginal dimensions to the boundary of the search space, even when their effect on the objective is negligible.

We propose BONSAI (Bayesian Optimization with Natural Simplicity and Interpretability) to address this gap. BONSAI is a lightweight post-processing layer that sits on top of any acquisition function. At each BO iteration t , BONSAI: 1) identifies a candidate \mathbf{x}_t^* that maximizes the acquisition function α_t , 2) defines the *acquisition gap* $\Delta_t(\mathbf{x}) = \alpha_t(\mathbf{x}_t^*) - \alpha_t(\mathbf{x})$ of any point \mathbf{x} at round t , 3) greedily resets components of \mathbf{x}_t^* back to their default values as long as the acquisition gap of the pruned candidate remains below a relative threshold, and 4) returns the pruned point $\tilde{\mathbf{x}}_t$ when any further one-component reset exceeds the relative threshold on the acquisition gap. Intuitively, BONSAI asks: which parts of the suggested change can be safely reverted to the default without materially affecting the acquisition value? Although BONSAI is implemented as a lightweight pruning step, it directly affects the queried points and is therefore part of the BO decision policy rather than a purely post-hoc analysis. BONSAI is designed to simplify recommendations throughout optimization: each suggested configuration is intended to be simple and interpretable relative to the default and to remain a plausible final recommendation if the optimization is stopped early. In settings where each trial is costly to run or to review, producing “always-simple” intermediate recommendations can be as important as simplifying the final deployment candidate.

Our design goals are threefold. First, BONSAI should make BO recommendations easier to interpret (a key requirement

for adoption in practice) by explicitly highlighting the minimal set of parameters that need to change relative to the status quo. Second, it should be easy to integrate with existing BO systems: BONSAI operates purely as a post-processing step and does not require modifying the surrogate or acquisition. Third, we would like to quantify—and, when desired, control—the extra regret that pruning introduces relative to standard BO.

Contributions.

1. We formalize the setting of *default-aware* BO, where the goal is not only to optimize a black-box function but also to minimize deviation from a specified default configuration, measured by the number of components that change.
2. We introduce BONSAI, a default-aware BO policy that modifies acquisition-maximizing candidates by reverting low-impact deviations to a user-specified default configuration while enforcing a gap rule on the decrease in acquisition value.
3. In the context of using the Upper Confidence Bound (UCB) acquisition function with a Gaussian Process surrogate, we prove that BONSAI’s regret is bounded by the usual GP-UCB term plus a sum of threshold-dependent penalties, the latter of which is controlled under a particular gap rule leading to sublinear regret.
4. We evaluate Expected Improvement (EI) and UCB variants of BONSAI on synthetic and real-world test problems, demonstrating that BONSAI yields favorable sparsity–performance trade-offs: it substantially reduces the number of non-default parameters in the recommended configurations while maintaining competitive optimization performance and wall time relative to standard BO.

2. Background

We briefly review Bayesian optimization (BO), Gaussian process (GP) surrogates, and the GP-UCB algorithm, focusing on the components used in our analysis. We refer to Appendix A and Srinivas et al. (2010) for full details.

Bayesian optimization and GP surrogates. We consider the problem of maximizing an unknown function $f : \mathbb{X} \rightarrow \mathbb{R}$ over a compact domain $\mathbb{X} \subset \mathbb{R}^d$. At iteration t , the algorithm selects a point $\mathbf{x}_t \in \mathbb{X}$, observes a noisy evaluation $y_t = f(\mathbf{x}_t) + \varepsilon_t$, where the noise $\varepsilon_t \sim \mathcal{N}(0, \sigma^2)$ and σ^2 is the noise variance, and uses the history $\{(\mathbf{x}_s, y_s)\}_{s=1}^t$ to decide where to evaluate next. A common choice of surrogate model is a GP prior over f with a constant mean and covariance function k . Conditioned on the data up to time $t-1$, the GP posterior has mean $\mu_{t-1} : \mathbb{X} \rightarrow \mathbb{R}$ and standard deviation $\sigma_{t-1} : \mathbb{X} \rightarrow \mathbb{R}_+$.

Acquisition functions. BO algorithms typically select \mathbf{x}_t by maximizing an *acquisition function* $\alpha_t : \mathbb{X} \rightarrow \mathbb{R}$ that quantifies the utility of evaluating f at \mathbf{x} given the current posterior. The acquisition balances *exploration* by preferring points with large posterior uncertainty and *exploitation* by preferring points with a large posterior mean. Popular choices include Expected Improvement (EI, Jones et al., 1998), which measures the expected positive improvement over the best observed value so far; Upper Confidence Bound (UCB, Srinivas et al., 2010), which takes the form $\alpha_t^{\text{UCB}}(\mathbf{x}) = \mu_{t-1}(\mathbf{x}) + \beta_t \sigma_{t-1}(\mathbf{x})$, where $\beta_t > 0$ controls the exploration–exploitation trade-off; and information-based criteria such as entropy search (Hennig & Schuler, 2012). In this paper, BONSAI itself is agnostic to the choice of acquisition function; it only requires the ability to evaluate $\alpha_t(\mathbf{x})$ at candidate points. For our theoretical analysis, we focus on UCB, while in our experiments we also apply BONSAI to EI, which is often more robust in practice (Jones et al., 1998; Shahriari et al., 2016).

3. Related Work

Conservative and safe bandits with baselines. A related line of work studies *conservative* or *safe* policies that constrain performance relative to a baseline arm or configuration, e.g., by requiring the cumulative reward not to fall too far below a status-quo level (e.g., Kazerouni et al., 2017; Sui et al., 2015). BONSAI is not a safety mechanism of this particular type: our constraint is imposed on the acquisition rather than on the unknown objective, and the primary goal is to simplify recommendations in input space rather than to provide outcome-level safety guarantees. We view these approaches as complementary, and BONSAI could be combined with conservative BO when both simplicity and outcome-level constraints are required.

Variable selection and shrinkage for high-dimensional BO. Other work exploits sparsity to improve BO in high dimensions. Methods such as SAASBO (Eriksson & Jankowiak, 2021) and VSBO (Shen & Kingsford, 2023) aim to identify a small set of influential dimensions via shrinkage priors on kernel lengthscales or forward-stage selection using importance scores. Hvarfner et al. (2024) propose a dimensionality-scaled hyperprior whose mean grows with \sqrt{d} , progressively shrinking lengthscales toward larger values as dimensionality increases. These techniques primarily target the structure of the objective f to improve sample efficiency. However, even when only a few dimensions are relevant, the recommended configuration can still deviate substantially from a practitioner-chosen default across many components. BONSAI instead measures complexity directly via the ℓ_0 distance to a user-specified default and prunes low-impact deviations regardless of whether they arise in globally relevant or irrelevant dimensions.

Explainable and interpretable BO. Recent work has begun to study the interpretability of BO recommendations. For example, Chakraborty et al. (2025) explain BO solutions by identifying tunable subspaces and quantifying parameter-wise contributions, and Adachi et al. (2024) explore techniques to make BO behavior more transparent to practitioners. BONSAI is complementary: rather than explaining a potentially complex recommendation in the full input space, it directly simplifies the recommendation by reverting as many components as possible to their default values while maintaining a near-optimal acquisition value. This can be useful both on its own and as a front-end to post-hoc explanation methods applied to the pruned suggestion.

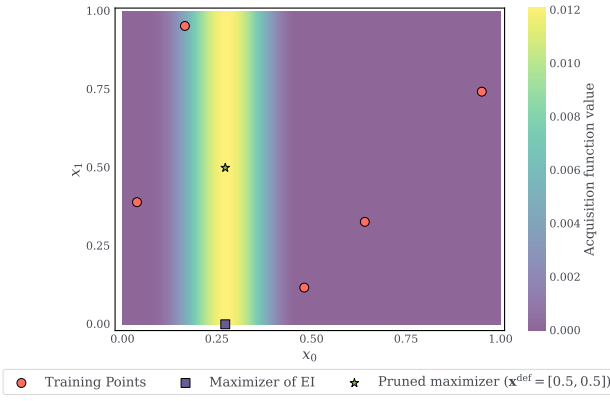


Figure 1. This figure shows an example where parameters that have no effect end up at the boundary value. Starting with 5 training points (orange dots) from the function $f(\mathbf{x}) = (x_0 - 0.25)^2$, a GP correctly infers that only x_0 is relevant for modeling f . Even though the effect of x_1 is close to zero numerically (the GP lengthscale for x_1 is long), the maximizing EI yields a candidate at the boundary (purple square). BONSAI mitigates this issue by moving the x_1 back to its default value (green star).

Sparse BO. SEBO (Liu et al., 2023) poses sparse Bayesian optimization, where the goal is to identify sparse *solutions* that deviate from a default configuration \mathbf{x}^{def} by learning trade-offs between sparsity and the objective. Our work is inspired by this perspective but differs in goal: rather than learning a sparsity–objective trade-off, we aim to optimize the objective while removing low-impact changes from the default. The internal and external regularization (IR and ER) methods of Liu et al. (2023) are most related. IR penalizes the objective by $\|\mathbf{x} - \mathbf{x}^{\text{def}}\|_0$, so improvements are measured with respect to a modified objective; this typically requires acquisition-specific modifications (which can be nontrivial, e.g., for multi-objective acquisition functions), limiting applicability. ER instead penalizes the acquisition function. Both approaches rely on a hard-to-tune regularization parameter and are non-differentiable due to the ℓ_0 term, making optimization challenging (e.g., even with homotopy continuation), and neither provides theoretical performance guarantees. In contrast, BONSAI is a simple and

computationally efficient post-processing procedure that is universally applicable and can provably recover sparse recommendations whose loss in acquisition value is bounded by an interpretable quantity.

BO with inexact acquisition maximization. Kim et al. (2025) analyze regret when the acquisition is not exactly maximized, which is useful for BONSAI since it can be viewed as inducing inexact acquisition maximization. However, Kim et al. (2025) do not consider inexact maximization as a mechanism for interpretability or simplifying recommendations.

See Appendix F for additional related work.

4. Methodology

We now formalize the default-aware BO setting and describe BONSAI. For clarity, we first consider a single BO iteration and suppress the time index on the acquisition function, writing $\alpha(\cdot)$ to denote the acquisition function in the current iteration. Each configuration $\mathbf{x} \in \mathbb{X} \subset \mathbb{R}^d$ represents a setting of d controllable input parameters, and we refer to x_j as the j -th component of the configuration.

4.1. Problem Setting

We assume the standard BO setting from Section 2. In addition we are given a fixed *default configuration* $\mathbf{x}^{\text{def}} \in \mathbb{X}$. Intuitively, \mathbf{x}^{def} represents the status quo: a configuration that has been vetted or previously deployed, and from which we prefer to deviate as little as possible. For the theoretical results in Section 5 and Appendix A we assume that $\mathbb{X} \subset \mathbb{R}^d$ is a compact hyper-rectangle and that each coordinate x_j is a real-valued input. In the experiments in Section 6, we also consider mixed continuous–discrete search spaces spaces; in that setting, we still index configurations by d components and interpret $\|\mathbf{x} - \mathbf{x}^{\text{def}}\|_0$ purely as the number of coordinates (continuous, integer, or categorical) in which \mathbf{x} differs from the default.

For a candidate $\mathbf{x} \in \mathbb{X}$ we define its *active set* $A(\mathbf{x}) := \{j \in \{1, \dots, d\} : x_j \neq x_j^{\text{def}}\}$, i.e., the components in which \mathbf{x} differs from the default. The number of changed components is then simply the ℓ_0 distance to the default, $\|\mathbf{x} - \mathbf{x}^{\text{def}}\|_0 = |A(\mathbf{x})|$. This quantity ignores the *magnitude* of the changes and only counts how many coordinates differ from the default, matching our goal of highlighting which parameters need to be touched at all. By definition, $A(\mathbf{x}^{\text{def}}) = \emptyset$.

Given a subset $S \subseteq \{1, \dots, d\}$, we write $P_S(\mathbf{x})$ for the configuration that keeps the components in S as in \mathbf{x} and

resets all others to their default values:

$$(P_S(\mathbf{x}))_j = \begin{cases} x_j, & j \in S, \\ x_j^{\text{def}}, & j \notin S. \end{cases}$$

When \mathbf{x} is a BO candidate and $S \subseteq A(\mathbf{x})$, $P_S(\mathbf{x})$ represents a pruned version of \mathbf{x} that changes only the components in S relative to the default \mathbf{x}^{def} .

Our ideal goal is to design, at each BO iteration, a selection rule that both (i) achieves near-maximal acquisition value and (ii) changes as few input parameters as possible relative to \mathbf{x}^{def} . Formally, one could pose a two-stage optimization problem: among all points whose acquisition lies within some tolerance of the maximum, choose the one with minimal ℓ_0 distance to the default. Solving this global combinatorial problem is intractable in general; BONSAI instead approximates it by finding an acquisition maximizer and considering variants of the maximizer that revert components to their default values. This is a local search around an acquisition maximizer. In particular, BONSAI only explores candidates of the form $P_S(\mathbf{x}_t^*)$ for subsets $S \subseteq \{1, \dots, d\}$; there may exist other near-optimal points close to \mathbf{x}^{def} in \mathbb{X} (e.g. if there are multiple maxima of the acquisition function) that are not reachable by this restricted local search, and BONSAI deliberately does not attempt to find them.

4.2. Acquisition Gaps and Thresholded Pruning

Let $\alpha : \mathbb{X} \rightarrow \mathbb{R}$ be the acquisition function at the current BO iteration, let $\mathbf{x}^* \in \arg \max_{\mathbf{x} \in \mathbb{X}} \alpha(\mathbf{x})$ be a maximizer (in practice approximated via numerical optimization). We define the *acquisition gap* of a point \mathbf{x} as $\Delta(\mathbf{x}) := \alpha(\mathbf{x}^*) - \alpha(\mathbf{x})$. This is the loss in acquisition value incurred by using \mathbf{x} instead of the maximizer \mathbf{x}^* .

BONSAI operates on the family of pruned candidates $\mathcal{X}^{\text{prune}} := \{P_S(\mathbf{x}^*) : S \subseteq A(\mathbf{x}^*)\}$, that is, all points obtained by resetting some subset of components of \mathbf{x}^* to their default values. For each such candidate, we can evaluate its acquisition gap $\Delta(P_S(\mathbf{x}^*))$. We introduce a *threshold* parameter $\rho \in [0, 1)$ that controls how far from the acquisition maximum we are willing to move. We use a relative gap rule where we accept pruned candidates whose acquisition gap is at most a fraction ρ of the maximum acquisition value.

Incremental Acquisition Functions To make the relative threshold well-posed and comparable across acquisitions, we apply it to an *incremental* acquisition value above a baseline. Specifically, we subtract the maximum acquisition value across the previously evaluated designs from the acquisition function $\tilde{\alpha}_t(\mathbf{x}) = \alpha_t(\mathbf{x}) - b_t$, where $b_t = \max_{s < t} \alpha_t(\mathbf{x}_s)$ before applying the relative rule.¹ For

¹We assume that there are always previously evaluated designs (e.g., a space-filling initialization before using BO.)

log-acquisition functions (Ament et al., 2023), we apply BONSAI to exponentiated acquisition values (undoing the log transform) before forming b_t and applying the relative rule: $\Delta(P_S(\mathbf{x}^*)) \leq \rho \tilde{\alpha}(\mathbf{x}^*)$, with $0 \leq \rho < 1$.

The set of admissible pruned candidates is

$$\mathcal{X}^{\text{feas}}(\rho) = \{\mathbf{x} \in \mathcal{X}^{\text{prune}} : \Delta(\mathbf{x}) \leq \rho \tilde{\alpha}(\mathbf{x}^*)\}. \quad (1)$$

We always have $P_{A(\mathbf{x}^*)}(\mathbf{x}^*) = \mathbf{x}^* \in \mathcal{X}^{\text{feas}}(\rho)$ since $\Delta(\mathbf{x}^*) = 0$. Within $\mathcal{X}^{\text{feas}}(\rho)$, BONSAI selects the candidate that deviates from the default in the fewest components: $\tilde{\mathbf{x}} \in \arg \min_{\mathbf{x}' \in \mathcal{X}^{\text{feas}}(\rho)} \|\mathbf{x}' - \mathbf{x}^{\text{def}}\|_0$. Equivalently, letting S range over subsets of $A(\mathbf{x}^*)$, we can write $\tilde{\mathbf{x}} = P_{S^*}(\mathbf{x}^*)$, where $S^* \in \arg \min_{S \subseteq A(\mathbf{x}^*)} \{|S| : \Delta(P_S(\mathbf{x}^*)) \leq \rho \tilde{\alpha}(\mathbf{x}^*)\}$.

In low dimensions we could, in principle, enumerate all subsets S and solve this combinatorial problem exactly. However, the number of subsets grows as $2^{|A(\mathbf{x}^*)|}$ and becomes prohibitive in high dimensions. BONSAI therefore uses a greedy algorithm that iteratively prunes components one at a time, exploring only those configurations that are reachable from \mathbf{x}^* by a sequence of single-component resets. Our focus on the family $\mathcal{X}^{\text{prune}}$ also means that BONSAI can miss pruned configurations that are not reachable via successive single-coordinate resets that maintain feasibility (for example, when two coordinates must be reset *jointly* to stay within the gap threshold). In our experiments on low-dimensional problems in Section 6 we find that this limitation has negligible effect on optimization performance.

4.3. Sequential Greedy Pruning

Below, we describe the sequential greedy variant of BONSAI used in our experiments (see Algorithm 1 in Appendix B for pseudocode). At round t , the inner optimizer finds \mathbf{x}_t^* . At round t , an inner optimizer returns \mathbf{x}_t^* (typically via approximate numerical maximization of the acquisition function). BONSAI then initializes $\tilde{\mathbf{x}}_t$ to \mathbf{x}_t^* and maintains the set \mathcal{D} of components where $\tilde{\mathbf{x}}_t$ differs from \mathbf{x}^{def} . Next, BONSAI considers resetting each component $j \in \mathcal{D}$ back to its default value and computes the acquisition gap g_j of the resulting candidate. Among the components for which the candidate satisfies the chosen gap rule, BONSAI picks the one with the smallest gap and performs the corresponding reset. The procedure stops once no further reset is feasible without violating the threshold. Our theoretical analysis in Section 5 treats \mathbf{x}_t^* as an exact maximizer and isolates the additional inexactness induced by pruning; Appendix A.1 notes how this composes with inner-solver accuracy.

By construction, the final $\tilde{\mathbf{x}}_t$ satisfies the relative gap condition at round t . Among all candidates reachable by successive single-component resets that respect the rule, BONSAI greedily removes the components that incur the smallest

drop in acquisition value at each step, often matching the exact combinatorial optimum in low dimensions (see Section 6). In high dimensions where enumerating all subsets is computationally infeasible, the greedy procedure provides a practical way to find an approximate solution to the problem of finding a candidate with near-maximal acquisition value with the fewest changes from the default point.

The additional computational cost of BONSAI compared to standard BO at iteration t arises from evaluating the acquisition on pruned candidates. In the worst case, BONSAI performs $O(d^2)$ acquisition evaluations per BO step: there are at most $|A(\mathbf{x}_t^*)| \leq d$ iterations of the outer while-loop, and each iteration considers up to $|\mathcal{D}|$ components. In many applications this overhead is modest relative to the cost of optimizing α_t itself or evaluating the underlying function f ; for very high-dimensional problems one can further reduce cost by subsampling components in \mathcal{D} at each step or restricting pruning to a subset of candidate dimensions.

5. Theoretical Analysis

In this section, we provide a theoretical analysis of BONSAI in the sequential setting, focusing on the GP-UCB acquisition. Complete proofs are provided in Appendix A.1.

Typically, the performance of a BO algorithm is measured in terms of the *instantaneous* and *cumulative* regret, which are given respectively by $r_t = f(\mathbf{x}^*) - f(\mathbf{x}_t)$ and $R_T = \sum_{t=1}^T r_t$, where $\mathbf{x}^* \in \arg \max_{\mathbf{x} \in \mathbb{X}} f(\mathbf{x})$. Under standard regularity assumptions on the objective and kernel (smoothness and boundedness conditions; see Appendix A and Srinivas et al. (2010)), GP-UCB enjoys sublinear cumulative regret: the average regret R_T/T goes to zero at a rate on the order of $\tilde{O}(\sqrt{\gamma_T/T})$, where γ_T is the usual maximum information gain. In Section 5.1, we provide the formal setup, and in Section 5.2, we express our bounds as this GP-UCB term plus an explicit, gap-dependent penalty.

Our goal is to make the connection to the classical GP-UCB results explicit and to separate what is specific to BONSAI from what is generic to *any* approximate UCB maximization scheme. The resulting bounds follow the standard GP-UCB analysis for the case of approximate maximization, tailored to the acquisition-gap perspective that BONSAI exposes.

The key observation is that the regret bounds we prove depend only on the *acquisition gaps* between the points actually queried by the algorithm and the ideal UCB maximizers. They do not depend on how those query points are constructed. BONSAI is one such construction that enforces bounded gaps while explicitly minimizing the number of deviations from a default configuration.

5.1. Preliminaries

We work in the standard GP-UCB setting of Srinivas et al. (2010) and adopt the standard GP-UCB assumptions: f lies in the reproducing kernel Hilbert space (RKHS) \mathcal{H}_k associated with a positive definite kernel k , with bounded norm $\|f\|_{\mathcal{H}_k} \leq B$, and the kernel variance is uniformly bounded so that $|f(\mathbf{x})| \leq \kappa B$ for all $\mathbf{x} \in \mathbb{X}$. We place a zero-mean GP prior with covariance k . Under these conditions, the GP posterior after $t-1$ observations has mean μ_{t-1} and standard deviation σ_{t-1} , and GP-UCB uses the acquisition function α_t^{UCB} defined in Section 2. As in the original GP-UCB analysis, we treat the kernel and noise hyperparameters as fixed and known when stating the guarantees; in practice they are typically learned from data.

We write $\mathbf{x}_t^* \in \arg \max_{\mathbf{x} \in \mathbb{X}} \alpha_t(\mathbf{x})$ and denote the maximum acquisition value by $\alpha_t^* := \alpha_t(\mathbf{x}_t^*)$. Following Kim et al. (2025), we define the (multiplicative) *acquisition accuracy* at round t as $\eta_t := \alpha_t(\tilde{\mathbf{x}}_t)/\alpha_t^* \in [0, 1]$, and the *worst-case accumulated inaccuracy* $M_T := \sum_{t=1}^T (1 - \tilde{\eta}_t) \in [0, T]$, where $\tilde{\eta}_t \leq \eta_t$ is any deterministic lower bound on the overall acquisition accuracy at round t (capturing both inner acquisition optimization and BONSAI’s pruning). Intuitively, $1 - \eta_t$ measures the (relative) loss in acquisition value at round t , and M_T aggregates these losses across time. To make BONSAI’s relative rule well-posed, we use the incremental acquisition $\tilde{\alpha}_t(\mathbf{x}) := \alpha_t(\mathbf{x}) - b_t$ with $b_t := \max_{s < t} \alpha_t(\mathbf{x}_s)$, and apply thresholds using $\tilde{\alpha}_t(\mathbf{x}_t^*) = \alpha_t^* - b_t$.

Our goal is to understand what happens when we allow a nonzero acquisition gap in order to simplify the recommended $\tilde{\mathbf{x}}_t$ relative to the default. The next subsection quantifies how this choice affects cumulative regret.

5.2. Regret Bounds for BONSAI with GP-UCB

We assume that at each round t the point $\tilde{\mathbf{x}}_t$ selected by the BO policy satisfies a gap rule relative to \mathbf{x}_t^* : $\Delta_t(\tilde{\mathbf{x}}_t) \leq \rho_t \tilde{\alpha}_t(\mathbf{x}_t^*)$ for some user-specified sequence $(\rho_t)_{t \geq 1}$, where $\rho_t \in [0, 1]$. Intuitively, ρ_t is the fraction of acquisition value we are willing to sacrifice at time t in order to simplify the configuration. We begin by bounding the accumulated acquisition inaccuracies in terms of ρ_t (Lemma A.1 in Appendix A.1). Leveraging this lower bound, we obtain the following regret bound for BONSAI with GP-UCB.

Theorem 5.1 (Regret bound via accumulated inaccuracy). *Assume the GP-UCB setting and kernel regularity conditions of Srinivas et al. (2010) and Kim et al. (2025): in particular, $f \in \mathcal{H}_k$ with $\|f\|_{\mathcal{H}_k} \leq B$, $k(x, x) \leq 1$, and the noise is conditionally R -sub-Gaussian. Let $\alpha_t(\mathbf{x}) = \mu_{t-1}(\mathbf{x}) + \beta_t \sigma_{t-1}(\mathbf{x})$ be the GP-UCB acquisition with $\beta_t = B + R \sqrt{2(\gamma_{t-1} + 1 + \log(1/\delta))}$, where $\delta \in (0, 1]$. Suppose that at round t BONSAI returns $\tilde{\mathbf{x}}_t$ satisfying the*

relative rule $\Delta_t(\tilde{\mathbf{x}}_t) \leq \rho_t \tilde{\alpha}_t(\mathbf{x}_t^*)$, where $\rho_t \in [0, 1]$. Let γ_T denote the maximum information gain after T evaluations. Then, with probability at least $1 - \delta$,

$$R_T = O\left(\sqrt{\gamma_T T} + \sqrt{\gamma_T} \sum_{t=1}^T \rho_t\right). \quad (2)$$

Intuitively, the cumulative regret is at most the regret of standard GP-UCB plus an additive penalty corresponding to the additional regret due to the accumulated inaccuracies. This gives a direct and interpretable trade-off: every time we insist on sparsity by potentially degrading the acquisition value by up to a fraction ρ_t , we pay a penalty proportional to ρ_t . Furthermore, BONSAI remains asymptotically no-regret under certain conditions on the sequence $(\rho_t)_{t \geq 1}$.

Corollary 5.2 (Asymptotic No-Regret). *If the relative thresholds satisfy $\sum_{t=1}^{\infty} \rho_t < \infty$ or more generally $\sum_{t=1}^T \rho_t = O(\sqrt{T})$, then BONSAI remains asymptotically no-regret and preserves the standard GP-UCB rate up to lower-order terms.*

For example, using $\rho_t = \frac{c}{t}$, where $c > 0$ satisfies Corollary 5.2 when used with squared exponential or Matérn kernels (see Corollary A.2 in Appendix A for formal examples and bounds).

These results align BONSAI with the inexact-maximization framework of Kim et al. (2025) and make the “cost of pruning” explicit: BONSAI enforces a per-round inexactness budget through ρ_t , which contributes additively to M_T and thus to the $M_T \sqrt{\gamma_T}$ term in the regret bound. By choosing a decreasing schedule (ρ_t) (e.g., $\rho_t \propto 1/t$), users can prune aggressively in early rounds while ensuring that the accumulated inaccuracy remains sublinear, so BONSAI retains the asymptotic optimality guarantees of exact GP-UCB.² Our primary theoretical contribution is quantifying the additional regret introduced by pruning (for both constant thresholds and decaying schedules), and we empirically validate that both constant and scheduled choices of ρ work well at the finite budgets of interest in Section 6 and Appendices C.7 and C.6.

5.3. Extensions

Batch candidate generation. In settings where multiple points are evaluated in parallel at each BO iteration, one typically maximizes a batch acquisition function $\alpha : \mathbb{X}^q \rightarrow \mathbb{R}$ over tuples $X = (\mathbf{x}_1, \dots, \mathbf{x}_q)$. BONSAI can be extended to this setting by applying the pruning procedure to each point in the batch while conditioning on the previously selected pruned batch entries. In the batch setting, we use the incremental acquisition function described in Section 4.2

²Wang & Jegelka (2017) showed that MES and PI are special cases of UCB, so our theoretical results hold for those as well.

when pruning the first point. For pruning subsequent points, we use the incremental improvement over the previously selected and pruned points in the batch.

Acquisition functions. Our theoretical results are specific to the GP-UCB acquisition. BONSAI itself, however, is purely a post-processing step that only requires the ability to evaluate an acquisition function at candidate points. In particular, it can be used with EI and its variants, which we find to be more robust in some of our empirical studies. In those cases, the regret guarantees in Section 5 should be viewed as a guide rather than a formal guarantee: they capture what happens if one could construct an acquisition function with analogous confidence properties and bounded gaps.

6. Experiments

We evaluate BONSAI on a variety of synthetic and real-world benchmark problems. We compare against the following baselines: quasi-random Sobol sampling, standard BO, and two methods for sparse BO, IR and ER (Liu et al., 2023). For IR/ER, we use a ℓ_0 penalty coefficient of 0.01, which is reported in SEBO as a strong default choice.³ See Appendix C.9 for a sensitivity analysis of IR and ER. All methods use the same MAP-SAAS GP surrogate: a GP with a Matérn-5/2 kernel with a SAAS prior (Eriksson & Jankowiak, 2021), where the GP hyperparameters are fit with a novel sampling and MAP estimation approach to speed up model fitting (see Appendix D for details).

We initialize each method by evaluating the default point \mathbf{x}^{def} and 20 Sobol samples. We leverage qLogNEI and qLogNEHVI (Ament et al., 2023) as the acquisition functions for all methods for single and multi-objective problems, respectively. For BONSAI, we use a fixed relative threshold $\rho = 0.2$ across all main-text experiments and provide a sensitivity analysis with respect to ρ in Appendix C.7. In Appendix C.6, we compare using EI to GP-UCB with a schedule on ρ_t proposed in Corollary A.2 and find comparable performance on most problems, with EI performing well across problems. All methods are implemented using Ax (Olson et al., 2025) with components from BoTorch (Balandat et al., 2020). BONSAI is implemented in Ax (Olson et al., 2025) and code is available at <https://github.com/facebook/Ax>.

6.1. Benchmarks

Our test problems include single-objective, constrained, and multi-objective settings. All problems are maximiza-

³IR and ER were proposed in Liu et al. (2023) for single-objective optimization, but we extend both to constrained optimization, and we extend ER to multi-objective optimization. See Appendix E for further discussion.

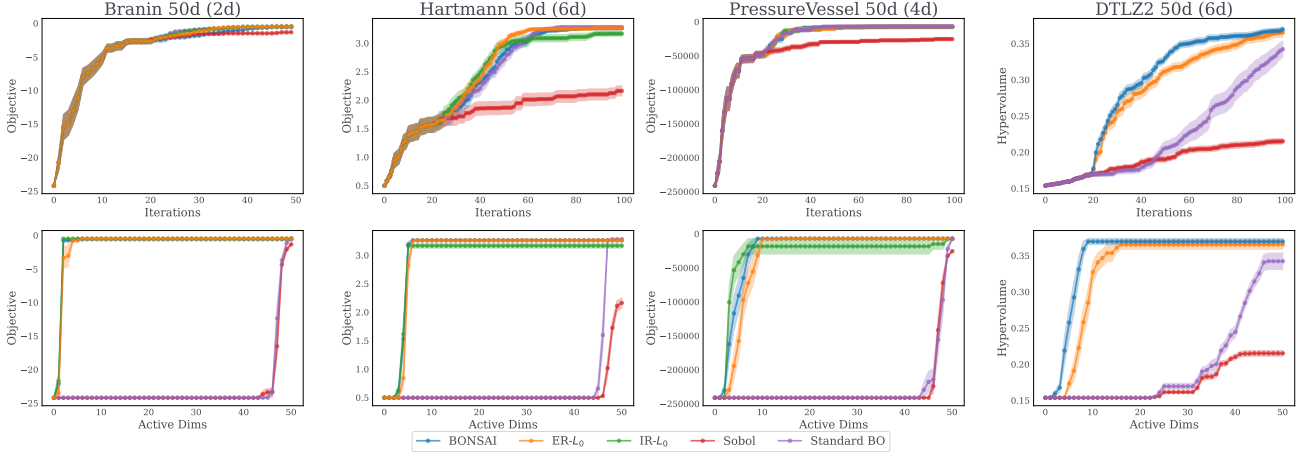


Figure 2. Top row: Objective or HV. Bottom row: Best Objective (or HV) value for each level of active dimensions. For MOO, HV is plotted against the average number of active dimensions across points in the Pareto frontier.

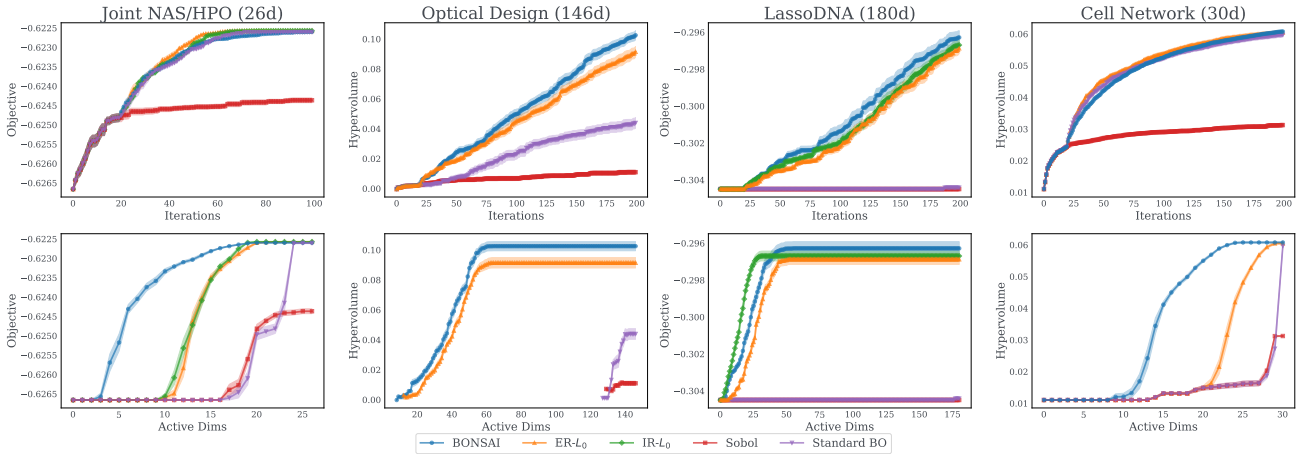


Figure 3. Top row: objective or HV. Bottom row: Best Objective (or HV) value for each level of active dimensions. For MOO, HV is plotted against the average number of active dimensions across points in the Pareto frontier.

tion problems—we negate the objective for minimization problems. We report optimization performance (best observed feasible objective for constrained problems and hypervolume (HV) for multi-objective problems) and candidate generation time—acquisition optimization and pruning (for BONSAI)—in sequential ($q = 1$) settings. See Appendix C.5 for results in batch ($q = 5$) settings. In all problems, we set \mathbf{x}^{def} to be the center of the search space, since the search space in real problems is often centered at the default configuration.

Synthetic Benchmarks. Each problem is embedded in a higher dimensional search space by adding extra irrelevant parameters. We set \mathbf{x}^{def} as the center of the search space. These problems include Branin (2d), Hartmann (6d), PressureVessel (4d, 4 constraints) (Coello Coello & Mezura Montes, 2002), and DTLZ2 (6d, 2-objective) (Deb et al., 2002), all embedded in 50d spaces. Additional results on lower-dimensional benchmarks are provided in Appendix C.

Joint NAS/HPO is a real-world joint neural architecture search and hyperparameter optimization problem originating from a multi-task, multi-label neural network model at a large web services firm. The problem has 26 parameters that include the widths and depths of different blocks (integer parameters) and initial weights for layer norms (continuous parameters). Training and evaluating the model is computationally intensive, so sample efficiency is paramount. For this benchmark, we leverage a GP surrogate fitted to data collected from a real optimization run.

Optical Design is a real-world problem where the goal is to optimize 146 continuous parameters that control the surface morphology and geometry of optical components of a see-through display for augmented reality (Daulton et al., 2022). The goal is to optimize two objectives: display efficiency and quality. Evaluating a design requires computationally intensive physical simulations; however, for the purposes of this benchmark, we leverage a neural network surrogate fit

to real data collected from optimization runs.

LassoDNA (Šehić et al., 2022) involves tuning 180 parameters (each in $[-1, 1]$) corresponding to the penalty for each feature in a weighted Lasso regression to minimize MSE on the DNA dataset (Chang & Lin, 2011).

Cell Network is a 30d optimization problem (Dreifuerst et al., 2021) where the goal optimize the transmission power (an integer in $\{0, \dots, 10\}$) and downtilt (a continuous parameter in $[30, 50]$) for each of 15 antennas in a cellular network to minimize two objectives: under-coverage and over-coverage.

See Appendix C for results on additional problems, including lower-dimensional problems and real-world ranking problems from a large web service (including noisy problems).

6.2. Results

We report optimization performance over the number of evaluations, the best objective found for a given number of active dimensions, and candidate generation time. For multi-objective problems, we report the hypervolume found versus the average active dimensions of the points in the Pareto set. We report the mean and ± 2 standard errors across 20 replications.

Across all benchmarks, we find that BONSAI yields consistently favorable sparsity–performance trade-offs: it produces substantially simpler recommendations while maintaining competitive performance with respect to the objective (or hypervolume), and it is typically the fastest default-aware method with respect to generation time. On synthetic benchmarks in Figure 2, we find that BONSAI recovers near-optimal solutions with very few active parameters—at or close to the true number of relevant parameters. While standard BO can achieve strong objective values in these settings, it typically does so via dense changes; in contrast, BONSAI focuses on the sparse-recommendation regime by construction and yields better objective values (or hypervolume) at comparable sparsity levels. IR and ER also find near-optimal sparse solutions, but IR fails to find the optimal solution on the Hartmann 50d problem, and BONSAI outperforms ER on DTLZ2 50d.

On the real problems in Figure 3, we find similar results. Interestingly, the real problems have significant numbers of irrelevant parameters; e.g., on the Optical Design problem, BONSAI finds excellent Pareto frontiers with an average of fewer than 60 active dimensions ($< 50\%$ of the parameters).

On DTLZ2, OpticalDesign, and LassoDNA, BONSAI performs better than standard BO, which we believe is due to BONSAI’s sparser candidates improving lengthscale estimation, as shown in Figure 17 in Appendix C.10.

Across all benchmarks, the candidate generation time (shown in Table 1 in Appendix C.1) of BONSAI is on-par with standard BO. IR and ER are typically much slower than BONSAI due to their use of homotopy continuation for acquisition optimization.

In Appendix C, we evaluate BONSAI on lower-dimensional synthetic benchmarks where all parameters are relevant and find that it performs on par with standard BO, highlighting the general applicability of BONSAI.

Greedy versus exact pruning. On low-dimensional synthetic problems, we additionally compare the sequential greedy BONSAI algorithm (Algorithm 1) to the exact combinatorial solution obtained by enumerating all subsets $S \subseteq A(x_t^*)$. As shown in Figure 11 in Appendix C.8, the sequential greedy algorithm performs comparably to exact pruning on low-dimensional problems, and exact pruning becomes slower as we increase the dimensionality (before becoming infeasible due to its exponential complexity with dimensionality).

7. Discussion

BONSAI is a technique for making BO recommendations simpler and more interpretable when a default configuration is available. By minimizing the number of deviations from the default, subject to an acquisition-gap constraint, BONSAI produces solutions that are easier to inspect, test, and deploy than unconstrained BO candidates, while reducing risks from system effects not captured by the objective.

Our analysis shows that, for GP-UCB, BONSAI can be viewed as a form of inexact acquisition maximization (Kim et al., 2025): if accumulated inaccuracy grows sublinearly, cumulative regret matches standard GP-UCB up to an additive penalty.

BONSAI measures simplicity via coordinate-wise ℓ_0 distance to the default, which is natural when parameters correspond to independently actionable knobs. In settings with correlated or grouped parameters, weighted or structured sparsity may be more appropriate; we view BONSAI as a first step in this direction. Empirically, greedy and exact pruning perform comparably, while greedy pruning is more scalable (Appendix C.8).

Future work includes deriving tighter sparsity guarantees, extending the analysis to acquisition functions such as EI, and combining BONSAI with post-hoc explanation methods to further improve transparency. See Appendix G for more directions for future work.

Impact Statement

This work aims to improve the usability and interpretability of Bayesian optimization in applications where there is a meaningful default configuration and where changing many parameters at once can be risky or costly from an operational perspective. By encouraging recommendations that change as few input parameters as possible relative to the default, BONSAI may help practitioners deploy BO in operationally constrained settings, such as large-scale systems configuration or model serving infrastructure.

At the same time, BONSAI is not a substitute for careful specification of objectives and constraints: if important aspects of system behavior are omitted from the optimization objective, BO—with or without BONSAI—may still propose configurations that are undesirable in practice. We therefore view BONSAI as a complementary tool that can make it easier for practitioners to inspect and reason about BO suggestions, but it should be used in conjunction with domain expertise, monitoring, and appropriate validation checks.

References

Adachi, M., Planden, B., Howey, D., A. Osborne, M., Orbell, S., Ares, N., Muandet, K., and Lun Chau, S. Looping in the human: Collaborative and explainable Bayesian optimization. In Dasgupta, S., Mandt, S., and Li, Y. (eds.), *Proceedings of The 27th International Conference on Artificial Intelligence and Statistics*, volume 238 of *Proceedings of Machine Learning Research*, pp. 505–513. PMLR, 02–04 May 2024. URL <https://proceedings.mlr.press/v238/adachi24a.html>.

Ament, S., Daulton, S., Eriksson, D., Balandat, M., and Bakshy, E. Unexpected improvements to expected improvement for bayesian optimization. In Oh, A., Naumann, T., Globerson, A., Saenko, K., Hardt, M., and Levine, S. (eds.), *Advances in Neural Information Processing Systems*, volume 36, pp. 20577–20612. Curran Associates, Inc., 2023.

Balandat, M., Karrer, B., Jiang, D. R., Daulton, S., Letham, B., Wilson, A. G., and Bakshy, E. BoTorch: A Framework for Efficient Monte-Carlo Bayesian Optimization. In *Advances in Neural Information Processing Systems 33*, 2020.

Chakraborty, T., Wirth, C., and Seifert, C. Explainable bayesian optimization, 2025. URL <https://arxiv.org/abs/2401.13334>.

Chang, C.-C. and Lin, C.-J. Libsvm: A library for support vector machines. *ACM Trans. Intell. Syst. Technol.*, 2(3), May 2011. ISSN 2157-6904. doi: 10.1145/1961189.1961199. URL <https://doi.org/10.1145/1961189.1961199>.

Coello Coello, C. A. and Mezura Montes, E. Constraint-handling in genetic algorithms through the use of dominance-based tournament selection. *Advanced Engineering Informatics*, 16(3):193–203, 2002. ISSN 1474-0346. doi: [https://doi.org/10.1016/S1474-0346\(02\)00011-3](https://doi.org/10.1016/S1474-0346(02)00011-3). URL <https://www.sciencedirect.com/science/article/pii/S1474034602000113>.

Daulton, S., Balandat, M., and Bakshy, E. Differentiable expected hypervolume improvement for parallel multi-objective bayesian optimization. In *Proceedings of the 34th International Conference on Neural Information Processing Systems*, NIPS ’20, Red Hook, NY, USA, 2020. Curran Associates Inc. ISBN 9781713829546.

Daulton, S., Balandat, M., and Bakshy, E. Parallel bayesian optimization of multiple noisy objectives with expected hypervolume improvement. In *Proceedings of the 35th International Conference on Neural Information Processing Systems*, NIPS ’21, Red Hook, NY, USA, 2021. Curran Associates Inc. ISBN 9781713845393.

Daulton, S., Eriksson, D., Balandat, M., and Bakshy, E. Multi-objective bayesian optimization over high-dimensional search spaces. In Cussens, J. and Zhang, K. (eds.), *Proceedings of the Thirty-Eighth Conference on Uncertainty in Artificial Intelligence*, volume 180 of *Proceedings of Machine Learning Research*, pp. 507–517. PMLR, 01–05 Aug 2022. URL <https://proceedings.mlr.press/v180/daulton22a.html>.

Daulton, S., Balandat, M., and Bakshy, E. Hypervolume knowledge gradient: A lookahead approach for multi-objective Bayesian optimization with partial information. In Krause, A., Brunskill, E., Cho, K., Engelhardt, B., Sabato, S., and Scarlett, J. (eds.), *Proceedings of the 40th International Conference on Machine Learning*, volume 202 of *Proceedings of Machine Learning Research*, pp. 7167–7204. PMLR, 23–29 Jul 2023. URL <https://proceedings.mlr.press/v202/daulton23a.html>.

Deb, K., Thiele, L., Laumanns, M., and Zitzler, E. Scalable multi-objective optimization test problems. volume 1, pp. 825–830, 06 2002. ISBN 0-7803-7282-4. doi: 10.1109/CEC.2002.1007032.

Dreifuerst, R. M., Daulton, S., Qian, Y., Varkey, P., Balandat, M., Kasturia, S., Tomar, A., Yazdan, A., Ponnampalam, V., and Heath, R. W. Optimizing coverage and capacity in cellular networks using machine learning. In *ICASSP 2021-2021 IEEE International Conference on Acoustics, Speech and Signal Processing*, 2021. URL <https://ieeexplore.ieee.org/abstract/document/9474710>.

Speech and Signal Processing (ICASSP), pp. 8138–8142. IEEE, 2021.

Eriksson, D. and Jankowiak, M. High-dimensional Bayesian optimization with sparse axis-aligned subspaces. In de Campos, C. and Maathuis, M. H. (eds.), *Proceedings of the Thirty-Seventh Conference on Uncertainty in Artificial Intelligence*, volume 161 of *Proceedings of Machine Learning Research*, pp. 493–503. PMLR, 27–30 Jul 2021. URL <https://proceedings.mlr.press/v161/eriksson21a.html>.

Feng, Q., Daulton, S., Letham, B., Balandat, M., and Bakshy, E. Experimenting, fast and slow: Bayesian optimization of long-term outcomes with online experiments. In *Proceedings of the 31st ACM SIGKDD Conference on Knowledge Discovery and Data Mining V.I*, KDD ’25, pp. 2235–2246, New York, NY, USA, 2025. Association for Computing Machinery. ISBN 9798400712456. doi: 10.1145/3690624.3709419. URL <https://doi.org/10.1145/3690624.3709419>.

Garnett, R. *Bayesian Optimization*. Cambridge University Press, 2023.

Hennig, P. and Schuler, C. J. Entropy search for information-efficient global optimization. *J. Mach. Learn. Res.*, 13 (null):1809–1837, June 2012. ISSN 1532-4435.

Hvarfner, C., Hellsten, E. O., and Nardi, L. Vanilla Bayesian optimization performs great in high dimensions. In Salakhutdinov, R., Kolter, Z., Heller, K., Weller, A., Oliver, N., Scarlett, J., and Berkenkamp, F. (eds.), *Proceedings of the 41st International Conference on Machine Learning*, volume 235 of *Proceedings of Machine Learning Research*, pp. 20793–20817. PMLR, 21–27 Jul 2024.

Hvarfner, C., Eriksson, D., Bakshy, E., and Balandat, M. Informed initialization for bayesian optimization and active learning. *arXiv preprint arXiv:2510.23681*, 2025.

Jones, D. R., Schonlau, M., and Welch, W. J. Efficient global optimization of expensive black-box functions. *Journal of Global Optimization*, 13:455–492, 1998.

Kazerouni, A., Ghavamzadeh, M., Abbasi-Yadkori, Y., and Van Roy, B. Conservative contextual linear bandits. In *Proceedings of the 31st International Conference on Neural Information Processing Systems*, NIPS’17, pp. 3913–3922, Red Hook, NY, USA, 2017. Curran Associates Inc. ISBN 9781510860964.

Kim, H., Liu, C., and Chen, Y. Bayesian optimization with inexact acquisition: Is random grid search sufficient? In Chiappa, S. and Magliacane, S. (eds.), *Proceedings of the Forty-first Conference on Uncertainty in Artificial Intelligence*, volume 286 of *Proceedings of Machine Learning Research*, pp. 2202–2222. PMLR, 21–25 Jul 2025. URL <https://proceedings.mlr.press/v286/kim25b.html>.

Lin, C.-H., Miano, J. D., and Dyer, E. L. Bayesian optimization for modular black-box systems with switching costs. In de Campos, C. and Maathuis, M. H. (eds.), *Proceedings of the Thirty-Seventh Conference on Uncertainty in Artificial Intelligence*, volume 161 of *Proceedings of Machine Learning Research*, pp. 1024–1034. PMLR, 27–30 Jul 2021. URL <https://proceedings.mlr.press/v161/lin21c.html>.

Liu, S., Feng, Q., Eriksson, D., Letham, B., and Bakshy, E. Sparse bayesian optimization. In Ruiz, F., Dy, J., and van de Meent, J.-W. (eds.), *Proceedings of The 26th International Conference on Artificial Intelligence and Statistics*, volume 206 of *Proceedings of Machine Learning Research*, pp. 3754–3774. PMLR, 25–27 Apr 2023. URL <https://proceedings.mlr.press/v206/liu23b.html>.

Olson, M., Santorella, E., Tiao, L. C., Cakmak, S., Eriksson, D., Garrard, M., Daulton, S., Balandat, M., Bakshy, E., Kashtelyan, E., Lin, Z. J., Ament, S., Beckerman, B., Onofrey, E., Igusti, P., Lara, C., Letham, B., Cardoso, C., Shen, S. S., Lin, A. C., and Grange, M. Ax: A platform for adaptive experimentation. In *AutoML 2025 ABCD Track*, 2025. URL <https://openreview.net/forum?id=U1f6wHtG1g>.

Sculley, D., Holt, G., Golovin, D., Davydov, E., Phillips, T., Ebner, D., Chaudhary, V., Young, M., Crespo, J.-F., and Dennison, D. Hidden technical debt in machine learning systems. In *Proceedings of the 29th International Conference on Neural Information Processing Systems - Volume 2*, NIPS’15, pp. 2503–2511, Cambridge, MA, USA, 2015. MIT Press.

Šehić, K., Gramfort, A., Salmon, J., and Nardi, L. Lassobench: A high-dimensional hyperparameter optimization benchmark suite for lasso. In *First Conference on Automated Machine Learning (Main Track)*, 2022. URL <https://openreview.net/forum?id=S4leJbTrLg5>.

Shahriari, B., Swersky, K., Wang, Z., Adams, R. P., and de Freitas, N. Taking the human out of the loop: A review of bayesian optimization. *Proceedings of the IEEE*, 104 (1):148–175, 2016. doi: 10.1109/JPROC.2015.2494218.

Shen, Y. and Kingsford, C. Computationally efficient high-dimensional bayesian optimization via variable selection. In Faust, A., Garnett, R., White, C., Hutter, F., and Gardner, J. R. (eds.), *Proceedings of the Second International Conference on Automated Machine Learning*, volume 224 of *Proceedings of Machine Learning Research*, pp. 1–10. PMLR, 2023. URL <https://proceedings.mlr.press/v224/shen23a.html>.

Learning Research, pp. 15/1–27. PMLR, 12–15 Nov 2023. URL <https://proceedings.mlr.press/v224/shen23a.html>.

Song, L., Xue, K., Huang, X., and Qian, C. Monte carlo tree search based variable selection for high dimensional bayesian optimization. In *Proceedings of the 36th International Conference on Neural Information Processing Systems*, NIPS ’22, Red Hook, NY, USA, 2022. Curran Associates Inc. ISBN 9781713871088.

Srinivas, N., Krause, A., Kakade, S., and Seeger, M. Gaussian process optimization in the bandit setting: No regret and experimental design. In *Proceedings of the 27th International Conference on International Conference on Machine Learning*, ICML’10, pp. 1015–1022, Madison, WI, USA, 2010. Omnipress. ISBN 9781605589077.

Sui, Y., Gotovos, A., Burdick, J., and Krause, A. Safe exploration for optimization with gaussian processes. In Bach, F. and Blei, D. (eds.), *Proceedings of the 32nd International Conference on Machine Learning*, volume 37 of *Proceedings of Machine Learning Research*, pp. 997–1005, Lille, France, 07–09 Jul 2015. PMLR. URL <https://proceedings.mlr.press/v37/sui15.html>.

Tay, S., Foo, C. S., Urano, D., Leong, R., and Low, B. K. H. Bayesian optimization with cost-varying variable subsets. In Oh, A., Naumann, T., Globerson, A., Saenko, K., Hardt, M., and Levine, S. (eds.), *Advances in Neural Information Processing Systems*, volume 36, pp. 3008–3031. Curran Associates, Inc., 2023.

Vakili, S., Khezeli, K., and Picheny, V. On information gain and regret bounds in gaussian process bandits. In Banerjee, A. and Fukumizu, K. (eds.), *Proceedings of The 24th International Conference on Artificial Intelligence and Statistics*, volume 130 of *Proceedings of Machine Learning Research*, pp. 82–90. PMLR, 13–15 Apr 2021. URL <https://proceedings.mlr.press/v130/vakili21a.html>.

Wang, Z. and Jegelka, S. Max-value entropy search for efficient Bayesian optimization. In Precup, D. and Teh, Y. W. (eds.), *Proceedings of the 34th International Conference on Machine Learning*, volume 70 of *Proceedings of Machine Learning Research*, pp. 3627–3635. PMLR, 06–11 Aug 2017. URL <https://proceedings.mlr.press/v70/wang17e.html>.

A. Proofs and Additional Theoretical Results

A.1. Proofs

Lemma A.1 (Relative rule implies accuracy lower bound). *Using BONSAI at round t , the acquisition accuracy satisfies $\eta_t \geq 1 - \rho_t$. Consequently we may take $\tilde{\eta}_t := 1 - \rho_t$ in the definition of M_T (assuming exact inner maximization), and the worst-case accumulated inaccuracy is bounded by $M_T \leq \sum_{t=1}^T \rho_t$.*

Proof. By definition,

$$\Delta_t(\tilde{\mathbf{x}}_t) = \alpha_t(\mathbf{x}_t^*) - \alpha_t(\tilde{\mathbf{x}}_t) \leq \rho_t \tilde{\alpha}_t(\mathbf{x}_t^*).$$

Recalling $\tilde{\alpha}_t(\mathbf{x}_t^*) = \alpha_t(\mathbf{x}_t^*) - b_t$ with $b_t := \max_{s < t} \alpha_t(\mathbf{x}_s) \geq 0$, we have

$$\Delta_t(\tilde{\mathbf{x}}_t) = \alpha_t(\mathbf{x}_t^*) - \alpha_t(\tilde{\mathbf{x}}_t) \leq \rho_t \alpha_t(\mathbf{x}_t^*),$$

and rearranging gives

$$\alpha_t(\tilde{\mathbf{x}}_t) \geq (1 - \rho_t) \alpha_t(\mathbf{x}_t^*).$$

Note that if $\alpha_t^* \leq 0$, BONSAI is not applied since $\Delta_t(\tilde{\mathbf{x}}_t) > 0$, meaning the relative rule is not satisfied. Hence, the inaccuracy is 0.

If $\alpha_t^* > 0$, dividing by $\alpha_t(\mathbf{x}_t^*) = \alpha_t^* > 0$ yields $\eta_t \geq 1 - \rho_t$, and thus $1 - \tilde{\eta}_t \leq \rho_t$ when we choose $\tilde{\eta}_t := 1 - \rho_t$. Summing over t proves the result. \square

Inner optimization accuracy. The argument above treats \mathbf{x}_t^* as an exact maximizer of α_t . If instead an inner solver returns $\hat{\mathbf{x}}_t$ with a guarantee $\alpha_t(\hat{\mathbf{x}}_t) \geq \eta_t^{\text{solve}} \alpha_t^*$ for some $\eta_t^{\text{solve}} \in (0, 1]$, and BONSAI is applied so that $\alpha_t(\tilde{\mathbf{x}}_t) \geq (1 - \rho_t) \alpha_t(\hat{\mathbf{x}}_t)$ on the same nonnegative acquisition scale, then the composite selection satisfies $\alpha_t(\tilde{\mathbf{x}}_t)/\alpha_t^* \geq (1 - \rho_t) \eta_t^{\text{solve}}$ and one may take $\tilde{\eta}_t = (1 - \rho_t) \eta_t^{\text{solve}}$ in the definition of M_T .

Theorem 5.1 (Regret bound via accumulated inaccuracy). *Assume the GP-UCB setting and kernel regularity conditions of Srinivas et al. (2010) and Kim et al. (2025): in particular, $f \in \mathcal{H}_k$ with $\|f\|_{\mathcal{H}_k} \leq B$, $k(x, x) \leq 1$, and the noise is conditionally R -sub-Gaussian. Let $\alpha_t(\mathbf{x}) = \mu_{t-1}(\mathbf{x}) + \beta_t \sigma_{t-1}(\mathbf{x})$ be the GP-UCB acquisition with $\beta_t = B + R\sqrt{2(\gamma_{t-1} + 1 + \log(1/\delta))}$, where $\delta \in (0, 1]$. Suppose that at round t BONSAI returns $\tilde{\mathbf{x}}_t$ satisfying the relative rule $\Delta_t(\tilde{\mathbf{x}}_t) \leq \rho_t \tilde{\alpha}_t(\mathbf{x}_t^*)$, where $\rho_t \in [0, 1]$. Let γ_T denote the maximum information gain after T evaluations. Then, with probability at least $1 - \delta$,*

$$R_T = O\left(\sqrt{\gamma_T T} + \sqrt{\gamma_T} \sum_{t=1}^T \rho_t\right). \quad (2)$$

Proof. This is a direct specialization of Theorem 3 of Kim et al. (2025) with $\rho_t = 1 - \eta_t$. Using the same exploration schedule β_t , yields (2). \square

Corollary 5.2 (Asymptotic No-Regret). *If the relative thresholds satisfy $\sum_{t=1}^{\infty} \rho_t < \infty$ or more generally $\sum_{t=1}^T \rho_t = O(\sqrt{T})$, then BONSAI remains asymptotically no-regret and preserves the standard GP-UCB rate up to lower-order terms.*

Proof. The asymptotic statement follows by comparing $\sum_{t=1}^T \rho_t$ to \sqrt{T} and using the known growth of γ_T for the kernels considered. \square

Corollary A.2 (Example schedules). *Assume $\gamma_T = O(\log^{d+1} T)$ (SE kernel) or $\gamma_T = O(T^{d/(d+2\nu)} \log^{2\nu/(2\nu+d)}(T))$ (Matérn kernel with smoothness $\nu > \frac{1}{2}$), as in Vakili et al. (2021). Let $\rho_t = \frac{c}{t^{1+\epsilon}}$, where $c > 0$ and $\epsilon > 0$. Then $\sum_{t=1}^{\infty} \rho_t < \infty$ and hence $M_T = O(1)$, so $R_T = O(\sqrt{\gamma_T T})$. More generally, if $\rho_t = c/t$ then $\sum_{t=1}^T \rho_t = O(\log T)$ and*

$$R_T = O\left(\sqrt{\gamma_T T} + \sqrt{\gamma_T} \log T\right),$$

which preserves the standard GP-UCB rate up to logarithmic factors. In both cases BONSAI's relative rule is gradually tightened over time (through decreasing ρ_t), which controls the growth of M_T and guarantees asymptotic optimality.

Proof. For $\rho_t = c/t^{1+\epsilon}$ with $\epsilon > 0$, the series $\sum_{t=1}^{\infty} \rho_t$ converges, so $M_T = O(1)$. Plugging into (2) yields

$$R_T = O(\sqrt{\gamma_T T} + \sqrt{\gamma_T}) = O(\sqrt{\gamma_T T}).$$

For $\rho_t = c/t$, we have $\sum_{t=1}^T \rho_t = c(1 + \log T)$, and (2) gives

$$R_T = O\left(\sqrt{\gamma_T T} + \sqrt{\gamma_T} \log T\right).$$

The growth of γ_T for SE and Matérn kernels then yields the stated asymptotics. \square

A.2. Thresholds and Acquisition Gaps: A Toy Additive Model

The regret bounds above characterize the optimization cost of allowing acquisition gaps, but they do not by themselves explain how the thresholds influence the *sparsity* of BONSAI's recommendations. We now give a brief, concrete picture of this interaction for a broad class of ARD kernels that includes both SE-ARD and Matérn-ARD (e.g., Matérn-5/2). This subsection helps explain which coordinates BONSAI tends to prune under common ARD kernels.

We assume an ARD kernel of the form

$$k(\mathbf{x}, \mathbf{x}') = \sigma_f^2 \phi(r(\mathbf{x}, \mathbf{x}')) , \quad r(\mathbf{x}, \mathbf{x}') = \sqrt{\sum_{j=1}^d \frac{(x_j - x'_j)^2}{\ell_j^2}},$$

where $\ell_j > 0$ are per-component lengthscales and $\phi : [0, \infty) \rightarrow \mathbb{R}$ is a smooth radial profile such that $r \mapsto r \phi'(r)$ is bounded on $[0, \infty)$. This family includes the SE-ARD kernel (with $\phi(r) = \exp(-\frac{1}{2}r^2)$) and common Matérn-ARD kernels such as Matérn-5/2.

Intuitively, large ℓ_j indicate directions along which the surrogate varies slowly, so we expect changes along those components to have a small effect on the acquisition. Under mild regularity conditions we can formalize this intuition by bounding the partial derivatives of the acquisition with respect to each coordinate.

Fix a round t and consider acquisition α_t and optimizer \mathbf{x}_t^* . Let $S_t^0 := \{j : x_{t,j}^* \neq x_j^{\text{def}}\}$ be the set of components where \mathbf{x}_t^* differs from the default. For any set of components $S \subseteq S_t^0$, define

$$R_S(\mathbf{x}_t^*) := P_{S_t^0 \setminus S}(\mathbf{x}_t^*),$$

that is, $R_S(\mathbf{x}_t^*)$ is the configuration obtained from \mathbf{x}_t^* by *resetting* the components in S to their default values and keeping all the others as in \mathbf{x}_t^* . Equivalently, $R_S(\mathbf{x}_t^*)$ corresponds to precisely pruning the components of S .

Let $\Delta_t(\mathbf{x}) = \alpha_t(\mathbf{x}_t^*) - \alpha_t(\mathbf{x})$ denote the acquisition gap at round t .

Assumption A.3 (Per-component acquisition gaps, toy model). For each $j \in S_t^0$ there exists $\Delta_{t,j} \geq 0$ such that the acquisition gap when only component j is reset satisfies

$$\Delta_t(R_{\{j\}}(\mathbf{x}_t^*)) \geq \Delta_{t,j}.$$

Moreover, we assume a simple subadditivity property:

$$\Delta_t(R_S(\mathbf{x}_t^*)) = \alpha_t(\mathbf{x}_t^*) - \alpha_t(R_S(\mathbf{x}_t^*)) \geq \sum_{j \in S} \Delta_{t,j}, \quad \forall S \subseteq S_t^0.$$

Assumption A.3 says that each component has an associated “individual gap” $\Delta_{t,j}$, and that the combined effect of resetting a set of components is at least the sum of their individual gaps. This rules out positive interaction effects in which resetting two components together could be cheaper than resetting them separately, and is best viewed as a simplified model for intuition rather than a realistic assumption in complex BO problems.

Let $S_t^{\text{prune}} \subseteq S_t^0$ denote the set of components that BONSAI resets to default at round t , so that $\tilde{\mathbf{x}}_t = R_{S_t^{\text{prune}}}(\mathbf{x}_t^*)$.

Proposition A.4 (Thresholds constrain how many high-impact components can be pruned). *Suppose Assumption A.3 holds at round t , and that the BONSAI applies the relative gap rule so that $\Delta_t(\tilde{\mathbf{x}}_t) \leq \rho_t \tilde{\alpha}_t(\mathbf{x}_t^*)$. Then*

$$\sum_{j \in S_t^{\text{prune}}} \Delta_{t,j} \leq \rho_t \tilde{\alpha}_t(\mathbf{x}_t^*).$$

In particular, if $\Delta_{t,j} \geq \Delta_{\min} > 0$ for all $j \in S_t^{\text{prune}}$, then

$$|S_t^{\text{prune}}| \leq \frac{\rho_t \tilde{\alpha}_t(\mathbf{x}_t^*)}{\Delta_{\min}}.$$

Proof. By construction, $\tilde{\mathbf{x}}_t$ is obtained from \mathbf{x}_t^* by resetting the components in S_t^{prune} to their default values, that is, $\tilde{\mathbf{x}}_t = R_{S_t^{\text{prune}}}(\mathbf{x}_t^*)$. Applying Assumption A.3 with $S = S_t^{\text{prune}}$ yields

$$\Delta_t(\tilde{\mathbf{x}}_t) = \Delta_t(R_{S_t^{\text{prune}}}(\mathbf{x}_t^*)) \geq \sum_{j \in S_t^{\text{prune}}} \Delta_{t,j}.$$

The relative gap rule implies $\Delta_t(\tilde{\mathbf{x}}_t) \leq \rho_t \tilde{\alpha}_t(\mathbf{x}_t^*)$, so

$$\sum_{j \in S_t^{\text{prune}}} \Delta_{t,j} \leq \tau_t.$$

If each $\Delta_{t,j} \geq \Delta_{\min}$, then

$$|S_t^{\text{prune}}| \Delta_{\min} \leq \sum_{j \in S_t^{\text{prune}}} \Delta_{t,j} \leq \rho_t \tilde{\alpha}_t(\mathbf{x}_t^*),$$

which proves the claimed bound. \square

Lemma A.5 (Coordinate sensitivity for ARD kernels). *Let α_t be the GP-UCB acquisition at round t with an ARD kernel of the form*

$$k(\mathbf{x}, \mathbf{x}') = \sigma_f^2 \phi \left(\sqrt{\sum_{j=1}^d \frac{(x_j - x'_j)^2}{\ell_j^2}} \right),$$

on a compact domain \mathbb{X} . Suppose that ϕ is differentiable with $r \mapsto r \phi'(r)$ bounded on $[0, \infty)$. Then there exists a constant $C_t < \infty$ (depending on the data, kernel hyperparameters, and β_t , but not on j) such that for all $\mathbf{x} \in \mathbb{X}$ and all $j \in \{1, \dots, d\}$,

$$\left| \frac{\partial \alpha_t(\mathbf{x})}{\partial x_j} \right| \leq \frac{C_t}{\ell_j}.$$

Proof. We sketch the argument. Differentiating the kernel with respect to the radial distance r gives

$$\frac{\partial k(\mathbf{x}, \mathbf{x}')}{\partial x_j} = \sigma_f^2 \phi'(r) \frac{\partial r}{\partial x_j}, \quad r = \sqrt{\sum_{m=1}^d \frac{(x_m - x'_m)^2}{\ell_m^2}}.$$

By the chain rule,

$$\left| \frac{\partial r}{\partial x_j} \right| = \frac{1}{r} \left| \frac{(x_j - x'_j)}{\ell_j^2} \right| \leq \frac{1}{\ell_j},$$

with the convention that the bound holds trivially at $r = 0$ by continuity. By assumption, $r \phi'(r)$ is bounded on $[0, \infty)$, and \mathbb{X} is compact, so both r and $\phi'(r)$ are bounded on $\mathbb{X} \times \mathbb{X}$. It follows that $|\partial k(\mathbf{x}, \mathbf{x}')/\partial x_j| \leq C'_k/\ell_j$ for some finite constant C'_k independent of j .

The GP posterior mean and variance are linear and quadratic forms in the kernel evaluations, respectively, with coefficients determined by the training data and the noise level. Differentiating those expressions with respect to x_j and applying the bound on $\partial k/\partial x_j$ shows that both $\partial \mu_{t-1}(\mathbf{x})/\partial x_j$ and $\partial \sigma_{t-1}(\mathbf{x})/\partial x_j$ are bounded in magnitude by C'_t/ℓ_j for some constant C'_t that depends on the data and hyperparameters but not on j . Since $\alpha_t(\mathbf{x}) = \mu_{t-1}(\mathbf{x}) + \sqrt{\beta_t} \sigma_{t-1}(\mathbf{x})$, we obtain the claimed bound with C_t proportional to $C'_t(1 + \sqrt{\beta_t})$. \square

Lemma A.5 implies that changing component j by $R_{t,j}$ can change the acquisition by at most $w_{t,j} := \frac{C_t R_{t,j}}{\ell_j}$, for some finite constant C_t that depends on the data, kernel hyperparameters, and β_t but not on j .

Now let $S \subseteq \{1, \dots, d\}$ be a set of components that we reset to their default values, and consider the candidate $\mathbf{x}' = P_S(\mathbf{x}_t^*)$, obtained by starting from \mathbf{x}_t^* and reverting the components in S back to \mathbf{x}^{def} . Resetting those components one at a time and summing the resulting changes in α_t yields the following bound on the acquisition gap:

$$\Delta_t(\mathbf{x}') = \alpha_t(\mathbf{x}_t^*) - \alpha_t(\mathbf{x}') \leq \sum_{j \in S} w_{t,j} = \sum_{j \in S} \frac{C_t R_{t,j}}{\ell_j}.$$

Under the relative gap rule with threshold ρ_t , any subset S satisfying $\sum_{j \in S} \frac{C_t R_{t,j}}{\ell_j} \leq \rho_t \tilde{\alpha}_t(\mathbf{x}_t^*)$ can therefore be reset to default while still respecting the relative constraint $\Delta_t(\tilde{\mathbf{x}}) \leq \rho_t \tilde{\alpha}_t(\mathbf{x}_t^*)$. In other words, $\rho_t \tilde{\alpha}_t(\mathbf{x}_t^*)$ acts as a per-round budget in the geometry induced by the ARD kernel: components with large lengthscales ℓ_j and small deviations $R_{t,j}$ incur little cost, while those with small ℓ_j and large $R_{t,j}$ can rapidly deplete the budget.

B. BONSAI Algorithm

Algorithm 1 BONSAI (sequential pruning with gaps)

```

1: Inputs: Acquisition functions  $(\alpha_t)_{t=1}^T$ , default  $\mathbf{x}^{\text{def}}$ , relative thresholds  $(\rho_t)_{t=1}^T$ 
2: for  $t = 1$  to  $T$  do
3:    $\mathbf{x}_t^* \approx \arg \max_{\mathbf{x} \in \mathbb{X}} \alpha_t(\mathbf{x})$ 
4:    $\tilde{\mathbf{x}}_t \leftarrow \mathbf{x}_t^*$ 
5:    $\mathcal{D} \leftarrow \{j : x_{t,j}^* \neq x_j^{\text{def}}\}$ 
6:    $b_t \leftarrow \max_{s < t} \alpha_t(\mathbf{x}_s)$  (with  $b_1 \leftarrow 0$ )
7:   Define  $\tilde{\alpha}_t(\mathbf{x}) \leftarrow \alpha_t(\mathbf{x}) - b_t$ 
8:   Define  $\Delta_t(\mathbf{x}) \leftarrow \alpha_t(\mathbf{x}_t^*) - \alpha_t(\mathbf{x})$ 
9:   while  $\mathcal{D} \neq \emptyset$  do
10:     $\text{gap}_{\text{best}} \leftarrow +\infty$ ,  $j_{\text{best}} \leftarrow -1$ 
11:    for  $j \in \mathcal{D}$  do
12:      Let  $\mathbf{x}' \leftarrow \tilde{\mathbf{x}}_t$  with component  $j$  reset to  $x_j^{\text{def}}$ 
13:       $g_j \leftarrow \Delta_t(\mathbf{x}')$ 
14:       $\text{feasible} \leftarrow (g_j \leq \rho_t \tilde{\alpha}_t(\mathbf{x}_t^*))$ 
15:      if  $\text{feasible}$  and  $g_j < \text{gap}_{\text{best}}$  then
16:         $\text{gap}_{\text{best}} \leftarrow g_j$ 
17:         $j_{\text{best}} \leftarrow j$ 
18:      end if
19:    end for
20:    if  $j_{\text{best}} \neq -1$  then
21:      Reset component  $j_{\text{best}}$  in  $\tilde{\mathbf{x}}_t$  to  $x_{j_{\text{best}}}^{\text{def}}$ 
22:       $\mathcal{D} \leftarrow \mathcal{D} \setminus \{j_{\text{best}}\}$ 
23:    else
24:      break
25:    end if
26:  end while
27:  Evaluate  $y_t = f(\tilde{\mathbf{x}}_t) + \varepsilon_t$ 
28:  Update the surrogate with  $(\tilde{\mathbf{x}}_t, y_t)$ 
29: end for

```

	BONSAI	ER- L_0	IR- L_0	SOBOL	STANDARD BO
BRANIN 50D (2D)	1.7 (± 0.1)	4.8 (± 0.6)	5.4 (± 0.7)	0.0 (± 0.0)	1.5 (± 0.1)
HARTMANN 50D (6D)	2.2 (± 0.2)	9.3 (± 0.9)	5.7 (± 0.3)	0.0 (± 0.0)	2.0 (± 0.1)
PRESSUREVESSEL 50D (4D)	25.1 (± 1.7)	35.2 (± 4.8)	40.3 (± 5.5)	0.0 (± 0.0)	17.3 (± 1.0)
DTLZ2 50D (6D)	7.8 (± 0.5)	23.9 (± 1.4)	—	0.0 (± 0.0)	6.4 (± 0.3)
JOINT NAS/HPO (26D)	3.5 (± 0.4)	125.3 (± 4.7)	118.0 (± 4.4)	0.0 (± 0.0)	4.5 (± 0.2)
OPTICAL DESIGN (146D)	33.1 (± 2.5)	49.3 (± 2.3)	—	0.1 (± 0.0)	21.2 (± 0.8)
LASSODNA (180D)	29.1 (± 2.7)	55.2 (± 4.8)	43.5 (± 3.4)	0.1 (± 0.0)	10.3 (± 0.8)
CELL NETWORK (30D)	18.0 (± 0.9)	445.1 (± 17.2)	—	0.0 (± 0.0)	15.7 (± 0.8)

Table 1. : The average candidate generation time in seconds per iteration for each problem (± 2 standard errors) across 20 replications. The fastest of the BO default-aware methods are shown in bold. BONSAI is the fastest default-aware method (within the uncertainty interval) on most problems and is typically much faster than IR or ER.

C. Additional Empirical Evaluation and Experiment details

C.1. Sequential Optimization Generation Times

As shown in Table 1, we find BONSAI has sequential generation times comparable to Standard BO and is significantly faster than the other default aware methods, IR and ER.

C.2. Method Details

For mixed search spaces (Cell Network and Joint NAS/HPO), we use Ax’s default dispatch to optimize the acquisition function using the mixed-alternating optimizer, which interleaves local search on the discrete parameters with L-BFGS-B steps on the continuous parameters (Olson et al., 2025) for all methods. The mixed-alternating optimizer makes IR and ER very slow as shown in the wall times on problems with discrete parameters (Cell Network and Joint NAS/HPO).

Priors on the GP hyperparameters are given in Appendix D.

For IR and ER, we use 30 steps in homotopy continuation, with $a_{\text{start}} = 0.2$ and $a_{\text{start}} = 10^{-3}$, which follows the recommendation in Liu et al. (2023).

For constrained problems, if there is no feasible previously evaluated point, we optimize the probability of feasibility as the acquisition function (as in Olson et al. (2025)) and do not perform pruning or leverage IR/ER.

C.3. Problem Details

LassoDNA is available at github.com/ksehic/LassoBench, and the DNA dataset is available under a BSD-3-Clause license via LIBSVM at github.com/cjlin1/libsvm.

C.4. Reference Points for MOO

For the OpticalDesign problem, we use a reference point of (1, 1) and normalize the objectives by dividing by the reference point, as in Daulton et al. (2022).

For CellNetwork, we use [0.35, 0.35] as the reference point.

For synthetic problems, we use default reference points for each in BoTorch (Balandat et al., 2020), which are commonly used in multi-objective Bayesian optimization papers (Daulton et al., 2020; 2021; 2023).

C.4.1. REAL-WORLD RANKING PROBLEMS

Const. Ranking is a real-world problem that consists of tuning 16 continuous parameters in a value model (Feng et al., 2025) used for ranking content on a major web service. The goal is to optimize one engagement metric while satisfying constraints on 2 other engagement metrics. Evaluating a design typically involves running A/B tests, which require significant time and consume experimentation resources. For this benchmark, we leverage a GP surrogate fit to data collected from real A/B tests. Observations are subject to additive zero-mean Gaussian noise, where the variance is that which was observed in the original A/B tests.

MOO Ranking is another value modeling tuning problem from a major web service, where there are 10 continuous parameters, and the goal is to learn the Pareto frontier between 2 engagement metrics. Again, we leverage a GP surrogate fit to data from real A/B tests (Feng et al., 2025).

Results The results for sequential optimization are shown in Figure 4. BONSAI finds near optimal solutions, with significantly fewer active dimensions than alternative methods. It is also significantly faster than IR and ER, as shown in Table 2.

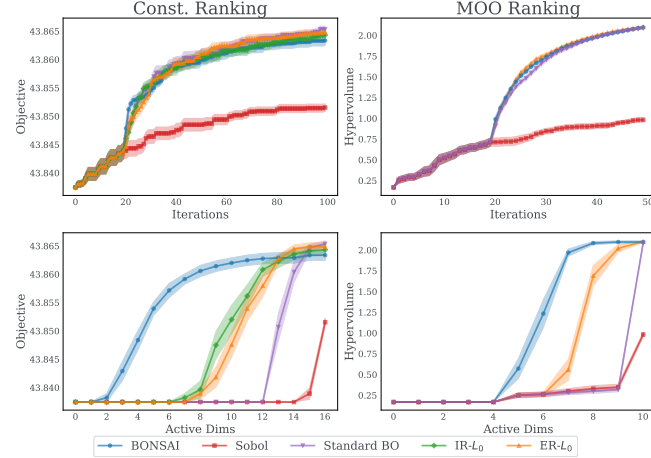


Figure 4. Real-world Ranking Problems. Top row: Objective or HV. Bottom row: Best Objective (or HV) value for each level of active dimensions. For MOO, HV is plotted against the average number of active dimensions across points in the Pareto frontier.

	BONSAI	ER-L ₀	IR-L ₀	SOBOL	STANDARD BO
CONST. RANKING	15.1 (± 2.4)	39.9 (± 6.1)	35.6 (± 4.0)	0.0 (± 0.0)	23.9 (± 2.9)
MOO RANKING	2.2 (± 0.1)	9.1 (± 0.3)	—	0.0 (± 0.0)	2.2 (± 0.1)

Table 2. : The average candidate generation time in seconds per iteration for each problem (± 2 standard errors) across 20 replications. The fastest of the BO default-aware methods are shown in bold. BONSAI is the fastest default-aware method (within the uncertainty interval) on most problems and is much faster than IR or ER.

C.5. Batch Optimization

We evaluate BONSAI in the batch setting where at each iteration, $q = 5$ points are generated. We find that BONSAI performs well in the batch setting too.

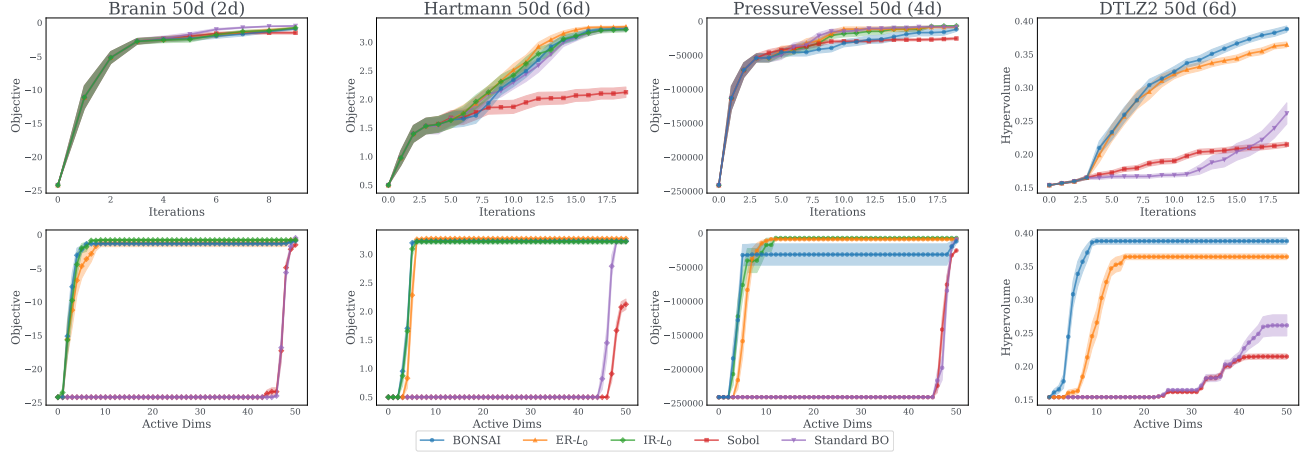


Figure 5. Optimization performance of BONSAI with batch optimization ($q = 5$) on synthetic problems. Top row: Objective or HV. Bottom row: Best Objective (or HV) value for each level of active dimensions. For MOO, HV is plotted against the average number of active dimensions across points in the Pareto frontier.

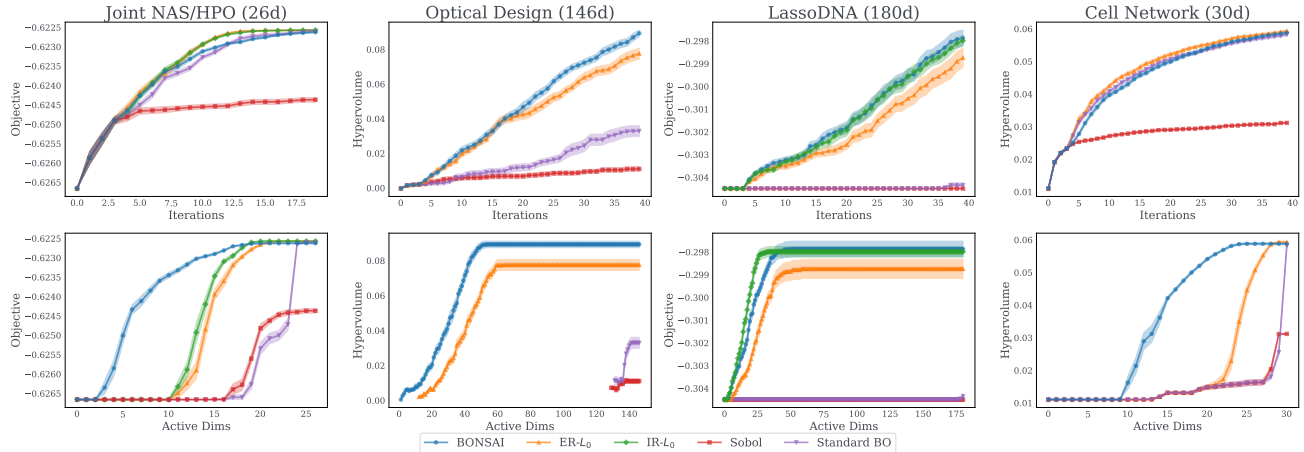


Figure 6. Optimization performance of BONSAI with batch optimization ($q = 5$) on real-world problems. Top row: Objective or HV. Bottom row: Best Objective (or HV) value for each level of active dimensions. For MOO, HV is plotted against the average number of active dimensions across points in the Pareto frontier.

	BONSAI	ER-L ₀	IR-L ₀	SOBOL	STANDARD BO
BRANIN 50D (2D)	8.5 (± 0.5)	18.4 (± 1.3)	16.4 (± 0.8)	0.0 (± 0.0)	7.8 (± 0.4)
HARTMANN 50D (6D)	12.9 (± 1.0)	43.3 (± 2.4)	29.1 (± 0.9)	0.0 (± 0.0)	8.7 (± 0.5)
PRESSUREVESSEL 50D (4D)	104.4 (± 7.2)	329.9 (± 16.4)	313.3 (± 15.9)	0.0 (± 0.0)	73.5 (± 3.8)
DTLZ2 50D (6D)	44.9 (± 1.3)	99.3 (± 4.3)	—	0.0 (± 0.0)	26.1 (± 1.2)
JOINT NAS/HPO (26D)	22.3 (± 0.5)	615.5 (± 20.2)	589.9 (± 14.1)	0.0 (± 0.0)	21.6 (± 0.6)
OPTICAL DESIGN (146D)	288.2 (± 15.8)	266.3 (± 11.5)	—	0.1 (± 0.0)	123.6 (± 2.8)
LASSODNA (180D)	159.8 (± 10.7)	144.6 (± 6.4)	104.7 (± 5.3)	0.1 (± 0.0)	69.3 (± 3.8)
CELL NETWORK (30D)	79.1 (± 3.1)	2060.5 (± 108.6)	—	0.0 (± 0.0)	83.9 (± 3.0)

Table 3. : The average batch generation time in seconds (generating batches of 5 points) for each problem (± 2 standard errors) across 20 replications. Generation time includes acquisition optimization and (when applicable) BONSAI pruning. The fastest of the BO default-aware methods are shown in bold. BONSAI is the fastest default-aware method (within the uncertainty interval) on most problems and is typically 2-3x faster than IR or ER.

C.6. BONSAI with UCB

We compare BONSAI (with qLogNEI) to BONSAI with UCB using a schedule on ρ_t proposed in Corollary A.2 with $c = 1$: $\rho_t = \frac{1}{t}$. We set the exploration parameter β_t in UCB to be $\beta_t = \sqrt{\log(t+2)}$ as in Kim et al. (2025). Figures 7 and 8 show that UCB performs similarly to EI on most problems, but UCB performs worse on LassoDNA. Since UCB is not applicable in multi-objective settings and EI acquisition functions (qLogNEI and qLogNEHVI) perform well across the board, we opt to use EI acquisition functions in our experiments.

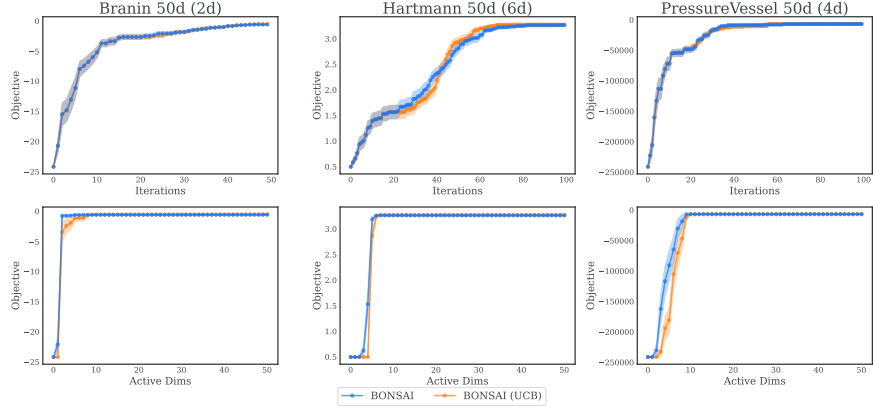


Figure 7. Comparison of BONSAI (with qLogNEI) to BONSAI with UCB on synthetic problems. Top row: Objective. Bottom row: Best Objective value for each level of active dimensions.

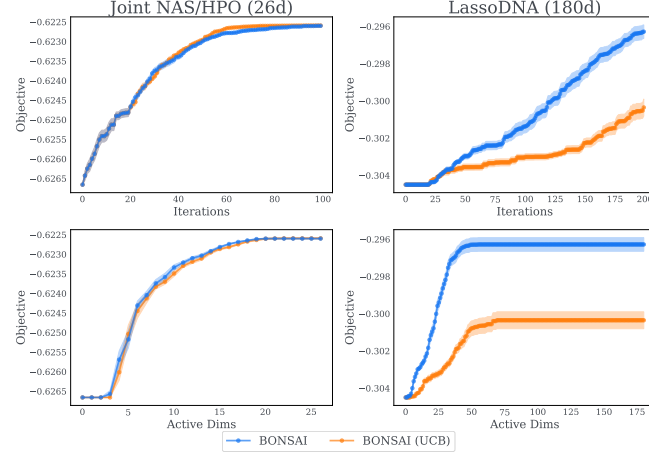


Figure 8. Comparison of BONSAI (with qLogNEI) to BONSAI with UCB on real-world problems. Top row: Objective. Bottom row: Best Objective value for each level of active dimensions.

C.7. Sensitivity with respect to ρ

We find that BONSAI is fairly robust with respect to the choice of ρ , as shown in Figures 9 and 10. We use $\rho = 0.2$ in the experiments in the main text.

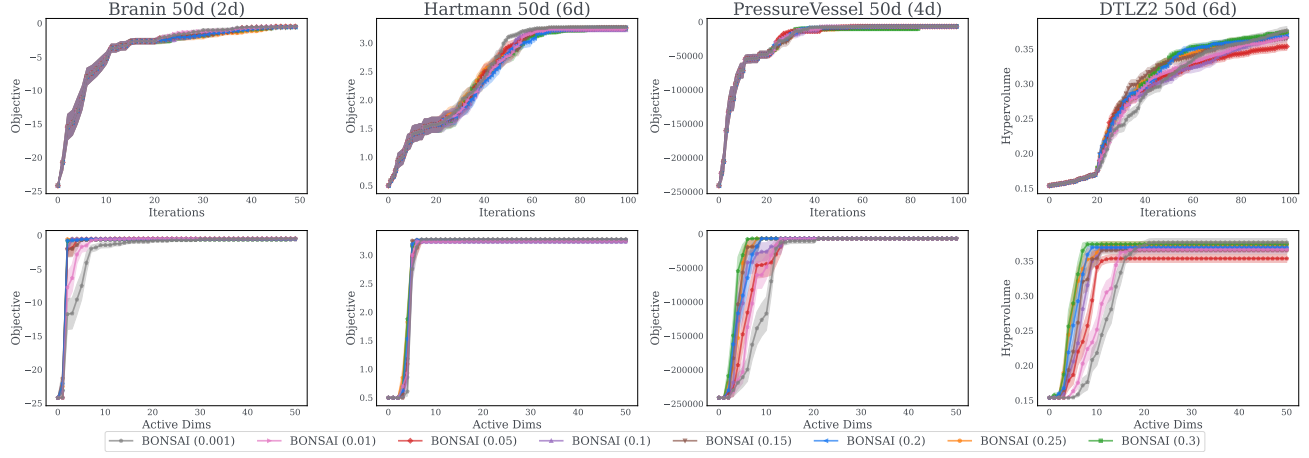


Figure 9. Top row: Objective or HV. Bottom row: Best Objective (or HV) value for each level of active dimensions. For MOO, HV is plotted against the average number of active dimensions across points in the Pareto frontier.

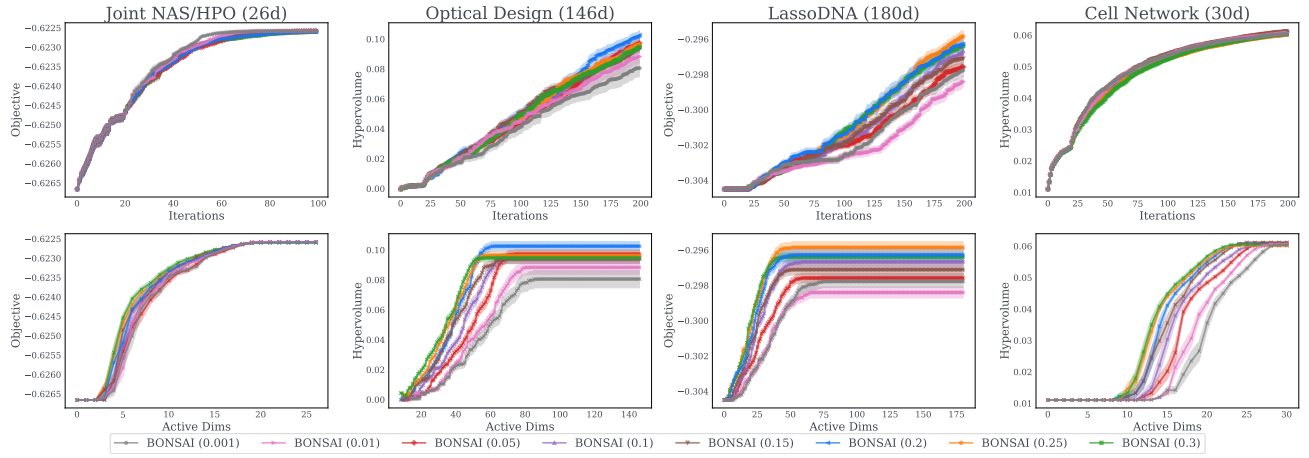


Figure 10. Top row: Objective or HV. Bottom row: Best Objective (or HV) value for each level of active dimensions. For MOO, HV is plotted against the average number of active dimensions across points in the Pareto frontier.

C.8. BONSAI with exact pruning

C.8.1. BONSAI WITH EXACT PRUNING FOR SEQUENTIAL OPTIMIZATION

In this section, we compare BONSAI with sequential greedy pruning to BONSAI with exact pruning. The performance of the two methods is comparable across problems, as shown in Figures 11 and 12, but BONSAI with sequential greedy pruning is significantly faster as the dimensionality increases (e.g., on Hartmann 15d and Branin 15d), as shown in Table 4. The complexity of exact pruning scales exponentially with the dimensionality, so it is only feasible to run exact pruning on relatively low dimensional problems. Across all 7 problems (and replicates of each) considered in this section, BONSAI with exact and sequential greedy pruning yield the same first candidate 85.7% of the time after the Sobol initialization. We compare the first point after the Sobol initialization since the models and acquisition functions are the same for BONSAI with exact and sequential greedy pruning at that point in time.

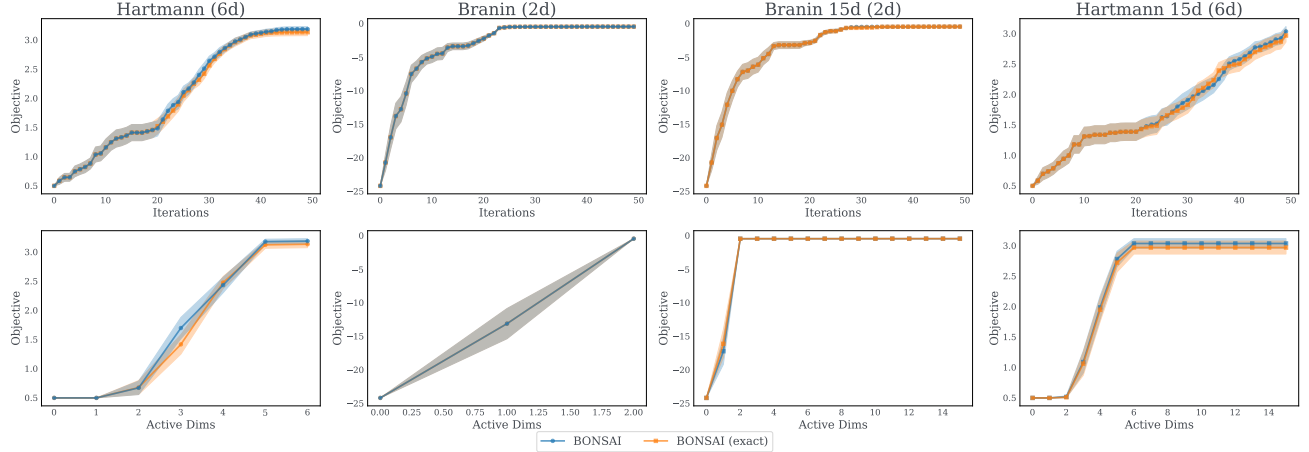


Figure 11. Optimization performance of BONSAI with exact and sequential greedy pruning with sequential optimization ($q = 1$). Top row: Objective or HV. Bottom row: Best Objective (or HV) value for each level of active dimensions. For MOO, HV is plotted against the average number of active dimensions across points in the Pareto frontier.

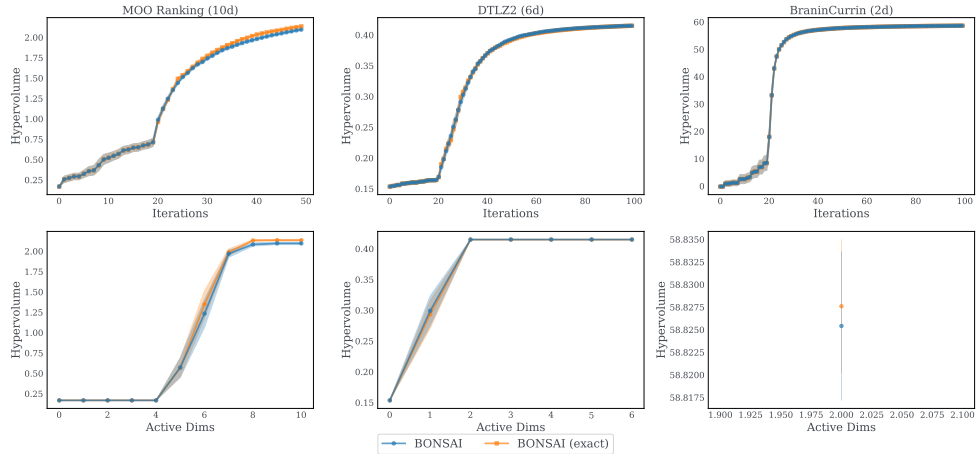


Figure 12. Optimization performance of BONSAI with exact and sequential greedy pruning with sequential optimization ($q = 1$). Top row: Objective or HV. Bottom row: Best Objective (or HV) value for each level of active dimensions. For MOO, HV is plotted against the average number of active dimensions across points in the Pareto frontier.

	BONSAI (EXACT)	BONSAI
HARTMANN (6D)	0.5 (± 0.0)	0.6 (± 0.0)
BRANIN (2D)	0.6 (± 0.1)	0.6 (± 0.1)
MOO RANKING (10D)	2.6 (± 0.1)	2.2 (± 0.1)
DTLZ2 (6D)	4.0 (± 0.2)	4.2 (± 0.1)
BRANINCURRIN (2D)	4.6 (± 0.5)	4.7 (± 0.3)
BRANIN 15D (2D)	2.0 (± 0.2)	1.2 (± 0.1)
HARTMANN 15D (6D)	1.4 (± 0.1)	0.7 (± 0.0)

Table 4. : The average candidate generation time per iteration in seconds for each problem (± 2 standard errors) across 20 replications. The fastest default-aware BO methods are shown in bold. BONSAI (with sequential greedy pruning) is significantly faster than BONSAI with exact pruning as the dimensionality increases (e.g., on Branin 15d and Hartmann 15d).

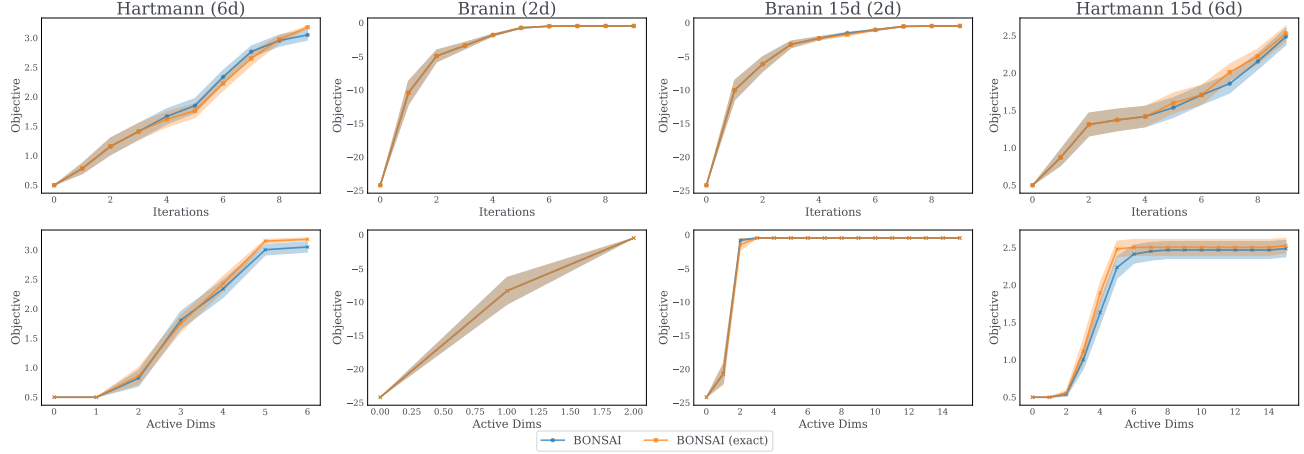
C.8.2. BONSAI WITH EXACT PRUNING FOR BATCH OPTIMIZATION ($q = 5$)


Figure 13. Optimization performance of BONSAI with exact and sequential greedy pruning with batch optimization ($q = 5$). Top row: Objective or HV. Bottom row: Best Objective (or HV) value for each level of active dimensions. For MOO, HV is plotted against the average number of active dimensions across points in the Pareto frontier.

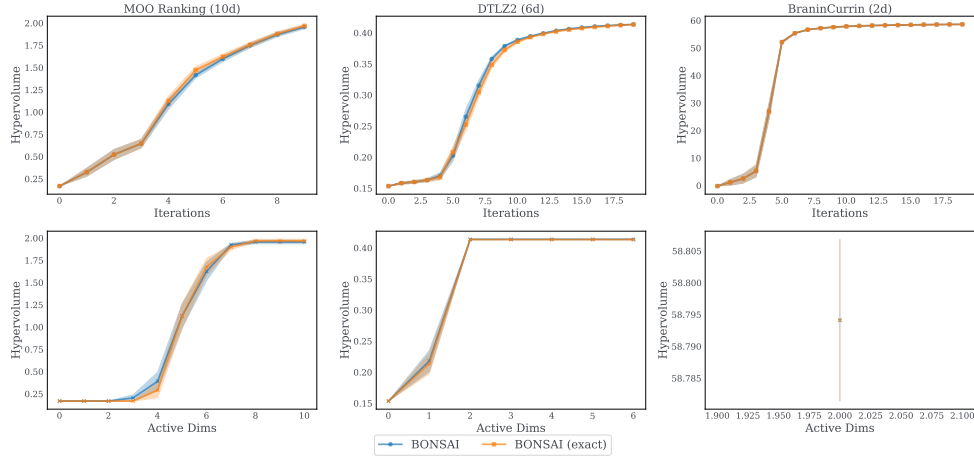


Figure 14. Optimization performance of BONSAI with exact and sequential greedy pruning with batch optimization ($q = 5$). Top row: Objective or HV. Bottom row: Best Objective (or HV) value for each level of active dimensions. For MOO, HV is plotted against the average number of active dimensions across points in the Pareto frontier.

	BONSAI (EXACT)	BONSAI
HARTMANN (6D)	2.9 (± 0.1)	2.9 (± 0.1)
BRANIN (2D)	2.7 (± 0.5)	2.7 (± 0.5)
MOO RANKING (10D)	11.7 (± 0.3)	10.0 (± 0.3)
DTLZ2 (6D)	17.5 (± 0.7)	17.3 (± 0.4)
BRANINCURRIN (2D)	25.0 (± 1.6)	24.7 (± 1.6)
BRANIN 15D (2D)	8.7 (± 0.3)	4.8 (± 0.3)
HARTMANN 15D (6D)	7.5 (± 0.2)	3.9 (± 0.2)

Table 5. : The average *batch* generation time per iteration (generating batches of 5 points) in seconds for each problem (± 2 standard errors) across 20 replications. The fastest default-aware BO methods are shown in bold. BONSAI (with sequential greedy pruning) is significantly faster than BONSAI with exact pruning as the dimensionality increases (e.g., on Branin 15d and Hartmann 15d).

C.8.3. DIMENSION SCALING PRIORS

All methods achieve less sparsity with dimension scaling priors (Hvarfner et al., 2024) than with MAP-SAAS. On problems with known numbers of active parameters, they do not find near-optimal solutions with the true number of active parameters. IR works slightly better than BONSAI on single-objective, problems, but BONSAI performs best on the multi-objective problem (DTLZ2). Importantly, the optimization performance of BONSAI relative to Standard BO is unaffected by changing the model class; rather, the difference is just the level of sparsity achieved by default-aware methods.

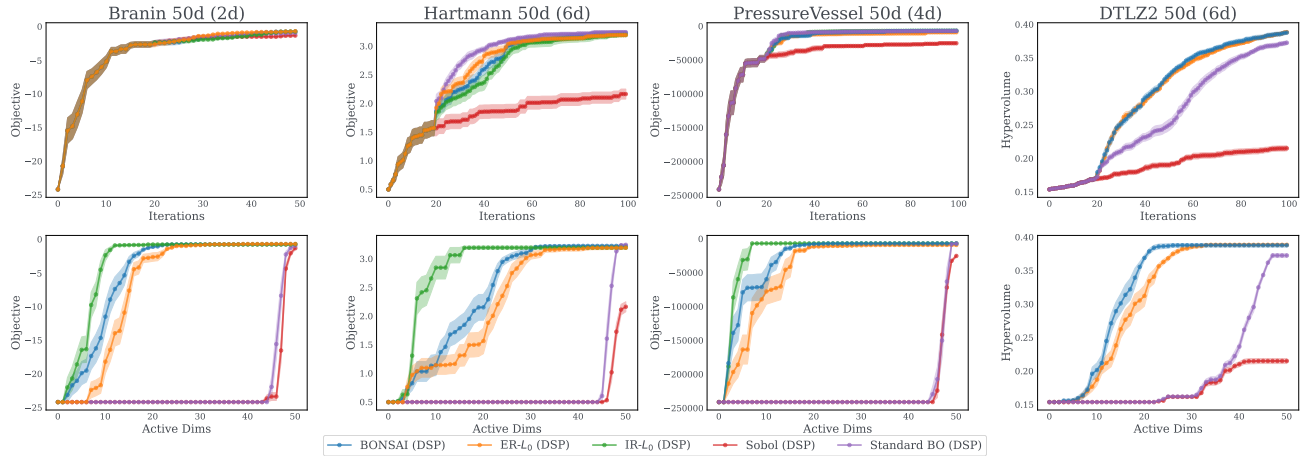


Figure 15. Sequential optimization performance of methods with a dimension-scaling prior (DSP). Top row: Objective or HV. Bottom row: Best Objective (or HV) value for each level of active dimensions. For MOO, HV is plotted against the average number of active dimensions across points in the Pareto frontier.

C.9. IR/ER Sensitivity Analysis

In our experiments, we set the penalty coefficient in IR and ER to be 0.01, which was a good default value from (Liu et al., 2023). In addition, we test different values of the penalty coefficient on synthetic problems to analyze the sensitivity of IR and ER. This analysis validates that 0.01 is a reasonable choice.

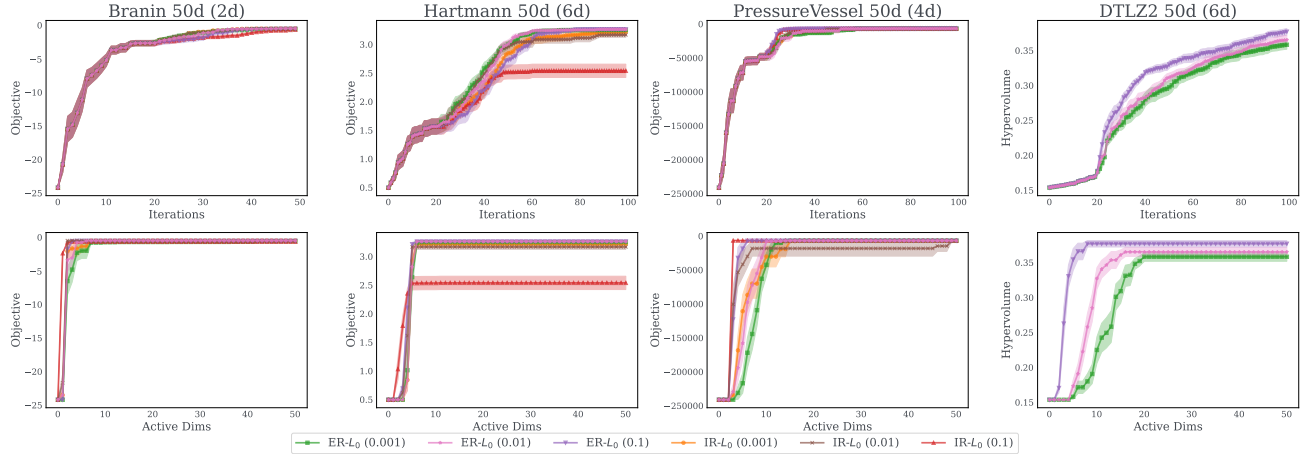


Figure 16. Top row: Objective or HV. Bottom row: Best Objective (or HV) value for each level of active dimensions. For MOO, HV is plotted against the average number of active dimensions across points in the Pareto frontier.

C.10. Improved Lengthscale Estimation

In this section we show that BONSAI improves the lengthscales estimation on the 6d DTLZ2 problem embedded in a 50d space. As illustrated in Figure 2, BONSAI outperforms Standard BO on this problem. Following (Hvarfner et al., 2025), we fit a GP with a dimension-scaling prior to the 100 trials collected by each replication of Sobol, Standard BO, and BONSAI. The distribution over replications of the log-lengthscales is illustrated in Figure 17.

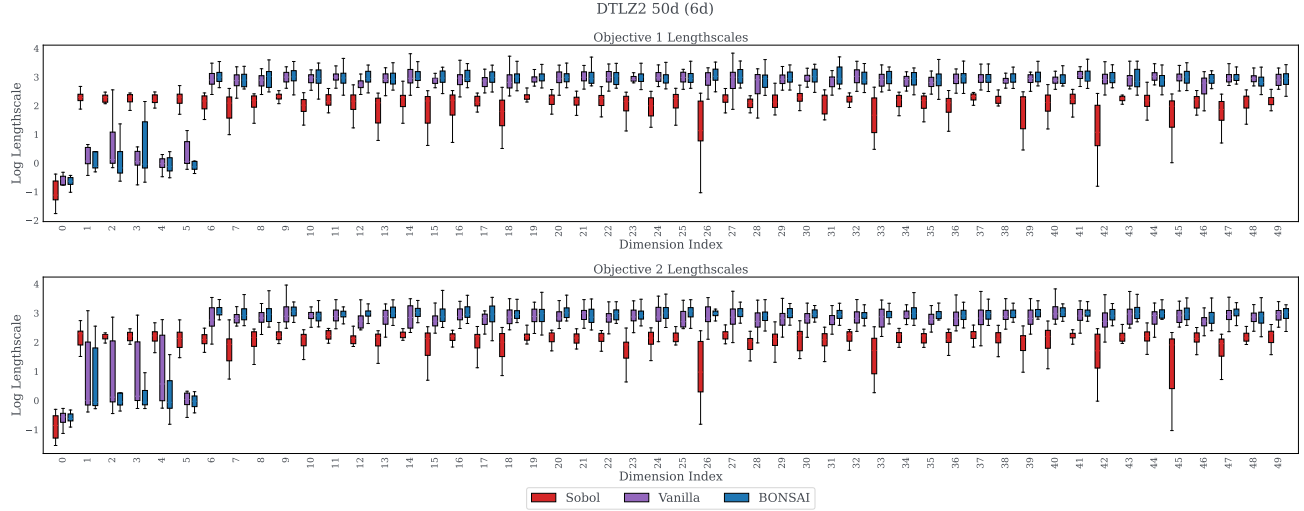


Figure 17. Estimated lengthscales using data collected by different methods on the DTLZ2 50d (6d) problem. Using the data collected by BONSAI consistently results in more accurate lengthscale estimation.

We observe that we are consistently able to identify the 6 non-redundant parameters when using the data collected by BONSAI. In comparison, using the data collected by Sobol and Standard BO results in sometimes failing to infer small lengthscales for the 6 non-redundant parameters, demonstrating that using pruning makes it easier for the underlying GP model to infer better lengthscales. We believe this is one of the reasons why BONSAI outperforms Standard BO on this problem.

D. MAP Estimation of SAASBO (MAP-SAAS)

To improve scalability relative to fully Bayesian SAASBO, we use an ensemble MAP approximation in which a small number of global sparsity scales are sampled and the remaining GP hyperparameters are fit via MAP. The fitting procedure

Algorithm 2 Ensemble MAP-SAAS GP

Require: Training data $X \in \mathbb{R}^{n \times d}$, $Y \in \mathbb{R}^{n \times 1}$
Require: Ensemble size $M \leftarrow 4$

- 1: Sample $\tau_1, \dots, \tau_M \stackrel{\text{iid}}{\sim} \text{HalfCauchy}(0.1)$
- 2: Form batched data $X^{(b)}, Y^{(b)} \in \mathbb{R}^{M \times n \times d}$
- 3: **for** $m = 1$ **to** M **do**
- 4: Define a Matérn-5/2 GP with ARD lengthscales $\ell_{m,1:d}$
- 5: Use priors: $\tau_m / \ell_{m,j}^2 \sim \text{HalfCauchy}(1.0)$, $\sigma_m^2 \sim \text{Gamma}(0.9, 10.0)$, $s_m \sim \text{Tophat}(10^{-2}, 10^4)$
- 6: Fit $\{\ell_{m,j}, \sigma_m^2, s_m\}$ by MAP
- 7: **end for**
- 8: Return a uniform Gaussian mixture posterior over ensemble members

is described in Algorithm 2. This ensemble construction approximates posterior uncertainty over sparsity patterns while retaining the computational efficiency of MAP-based GP fitting. For each model in the ensemble, we use a $\text{Tophat}(10^{-2}, 10^4)$ prior over the signal variance s_m and a $\text{Gamma}(0.9, 10.0)$ prior over the noise variance σ_m^2 .

Additionally, we compare BONSAI with MAP-SAAS to BONSAI with a GP with a dimension-scaling prior (DSP) (Hvarfner et al., 2024) and SAASBO (Eriksson & Jankowiak, 2021) and find that MAP-SAAS induces more sparsity.

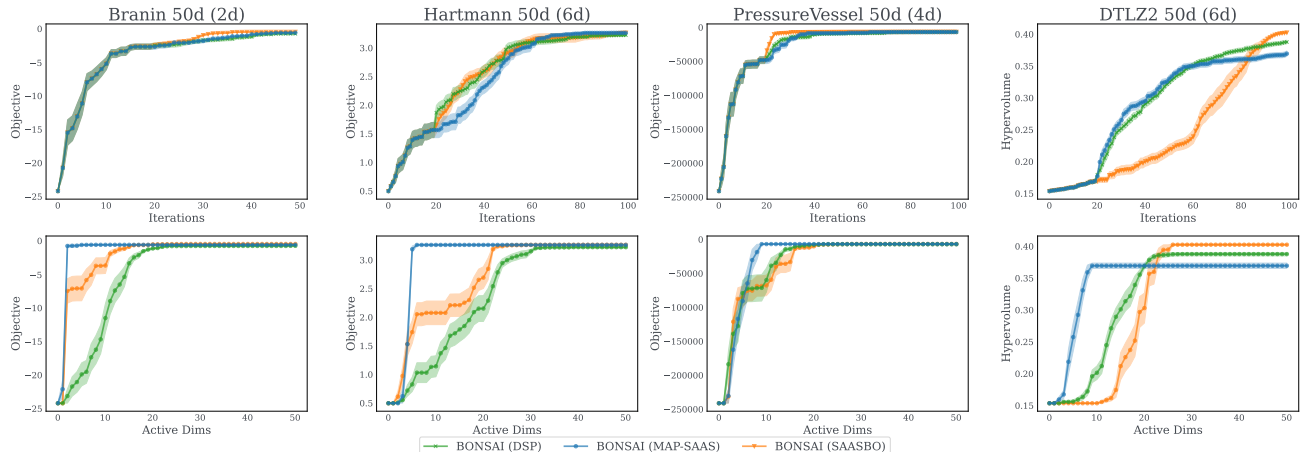


Figure 18. Sequential optimization performance of BONSAI with MAP-SAAS and the dimension-scaling prior. Top row: Objective or HV. Bottom row: Best Objective (or HV) value for each level of active dimensions. For MOO, HV is plotted against the average number of active dimensions across points in the Pareto frontier.

E. Extensions of IR and ER

IR can be extended to constrained qLogNEI in a straightforward way, since IR changes the objective by adding a penalty term based on the ℓ_0 -norm. Similarly, ER is can also be extended to constrained qLogNEI since the penalty in ER is simply added to the acquisition function externally.

Extending IR to multi-objective problems is non-trivial. For IR, one could penalize each objective by the sparsity penalty, but that would have a multiplicative effect on the hypervolume. Alternatively, one could subtract the sparsity penalty from the hypervolume of a set of points, but that would require extending the penalty to apply to sets of points. The issues of scale between hypervolume and the sparsity penalty may make it difficult to choose a reasonable value of the sparsity penalty coefficient.

F. Additional Related Work

Cost-aware and switching-cost Bayesian optimization. Several works incorporate explicit costs into BO. Cost-aware BO methods modify the acquisition to trade off reward and cost, or to preferentially query cheap configurations; see, e.g., work on cost-varying or subset-aware BO (Tay et al., 2023; Song et al., 2022). Lin et al. (2021) consider modular black-box systems in which changing components incurs switching costs and optimize a cost-augmented objective. BONSAI differs from these approaches in two ways. First, it does not require specifying or learning a cost function over individual input parameters. Instead, it enforces a hard constraint on the *acquisition gap* relative to the maximizer and, within that constraint, explicitly prefers the candidate with the fewest deviations from a fixed default configuration. Second, BONSAI is implemented as a post-processing step, leaving the underlying surrogate and acquisition function unmodified, and can thus be straightforwardly applied across a broad range of settings.

G. Future Work

In this section, we discuss directions for future work.

BONSAI measures simplicity using coordinate-wise ℓ_0 distance to the default, which is appropriate when each coordinate corresponds to a semantically meaningful and independently actionable knob. When parameters are correlated or meaningful only as groups (common in systems tuning), a grouped or weighted sparsity notion can be more realistic; we view BONSAI as a first step toward such structured pruning. Empirically, we also compare against exact pruning, which can reset multiple knobs simultaneously in one-shot and is capable of group-level pruning, and we find similar performance to sequential greedy pruning (Appendix C.8).

There are several directions for future work. First, it would be useful to develop tighter sparsity guarantees that move beyond the simplified per-component perspective in Section A.2 and to better characterize when greedy pruning matches the combinatorial optimum. Second, extending the theoretical analysis to EI and additional acquisition functions would require new tools, since the current proof techniques rely on confidence bounds. Third, it would be interesting to integrate BONSAI with more sophisticated models of user or operator preferences, for example allowing different components to have different “weights” in the ℓ_0 cost or incorporating structured defaults (such as grouped parameters). Finally, combining BONSAI with post-hoc explanation methods may further improve the transparency of BO-driven decision-making in practice.